1996

Reduction of high-speed impact transient data from a piezoelectric transducer

Rubâen T. Huerta-Ochoa
Lehigh University

Huerta-Ochoa, Rubén T.

Reduction of High-Speed Impact Transient Data from a Piezoelectric...

June 2, 1996

Reduction of High-Speed Impact Transient Data from a Piezoelectric Transducer

by

Rubén T. Huerta-Ochoa

A Thesis

Presented to the Graduate and Research Committee

of Lehigh University

in Candidacy for the Degree of

Master of Science

in

Mechanical Engineering

Lehigh University

April 8, 1996

This thesis is accepted and approved in partial fulfillment of the requirements for the Master of Science.

30 APRIL 1996

Date

Thesis Advisor

Chairperson of the Department

Acknowledgments:

I wish to thank Dr. Stanley H. Johnson for giving me the opportunity to learn about impact dynamics under his guidance. Also, I want to express my gratitude to the National Council of Science and Technology (CONACyT, Mexico) and to the Institute of International Education in Mexico City, for providing me a unique opportunity to pursue graduate studies in the United States of America. This work is especially dedicated to Rogerio Carranco Guzman, on his passing.

Table of Contents.

Abstract 1

1 Introduction 2

1.1 Historical background 2

1.2 Motivation for the study of impact processes 3

1.3 The piezoelectric transducer apparatus 4

2 Impact force measurement with a piezoelectric transducer 7

2.1 Problem statement 7

2.2 Scope of this thesis 8

3 Setting up the model for the transducer under impact 11

3.1 Sampling the impact process measurements 11

3.2 The ARMA model for the transducer dynamics 13

3.3 Modeling the presence of noise in the measurements 15

3.4 Outline of the identification procedure 18

4 Finding the system order 22

4.1 The concept of observability for a dynamical system 22

4.2 The identifiability condition for an unforced system 24

4.3 Order determination from samples of the impulse response 25

5 Finding periodicities in the transducer vibrations 30

5.1 The autorregressive law for the transducer free dynamics 30

5.2 A preliminary AR estimation by ordinary least squares 32

5.3 Improving the AR parameters by iteration 34

6 Reconstruction of phase and amplitude for the transducer dynamics 39

6.1 Relationship between AR and MA parameters 39

6.2 Estimation of the required first Markoff parameters 41

6.3 Overall model gain adjustment and deconvolution 45

6.4 Synopsis of the identification and deconvolution processes 46

7 Numerical results and discussion 47

7.1 Model identification for normal and transverse phenomena 47

A System order estimation for the normal and transverse models 49

B System identification of the normal model 50

C System identification of the transverse model 54

7.2 Results after filtering the vibrations: impact forces in the transducer 58

A Normal impact forces 59

B Transverse impact forces 64

8 Conclusions and future research 70

8.1 Summary of conclusions 70

8.2 Future research 71

References 74

Appendix A Experimental method 78

Vita 82

Table of Figures:

1.1 The piezoelectric transducer structure 6

2.1 The projectile-piezoelectric transducer impact 8

3.1 Block diagram for the complete transducer model 17

3.2 Two independent models for normal and transverse phenomena 18

5.1 Block diagram for the AR-prewhitening filter implementation 37

6.1 Synopsis of the Identification and Deconvolution Methodology 46

7.1 Typical normal vibration measurements 48

7.2 Typical transverse vibration measurements 48

7.3 System order estimation

(a) Normal impact model 49

(b) Transverse impact model 49

7.4 Fourier spectra before and after filtering normal measurements 50

7.5 Evolution of AR polynomial coefficients. (Normal impact) 51

7.6 Fourier spectra before and after filtering transverse measurements 54

7.7 Evolution of AR polynomial coefficients.(transverse impact) 55

7.8 Definition of an auxiliary fictitious impulse response

(transverse identification) 56

7.9 Backward in time propagation for the fictitious impulse response 58

7.10 Normal impact forces ($\alpha = 15$ degrees) 59

7.11 Normal impact forces (α =25 degrees) 60

7.12 Normal impact forces (α =35 degrees) 61

7.13 Normal impact forces (α =45 degrees) 61

7.14 Calculated vs. measured change in normal momentum 63

7.15 Transverse impact forces (Vin = 30.48m/s) 64

7.16 Transverse impact forces (Vin = 36.57m/s) 65

7.17 Transverse impact forces (Vin = 36.57m/s) 66

7.18 Transverse impact forces (Vin = 42.67m/s) 66

7.19 Calculated vs. measured change in transverse momentum 67

A.1 Definition of variables 77

A.2 Measurement of velocity 78

A.3 Measurement of trajectory angles 79

A.4 Measurement of spin rate 80

Abstract

The present work is concerned about the investigation of impact forces. Sampled measurements are taken from the transient behavior of a piezoelectric transducer under impact, and they are processed in order to infer the impact forces that produced these dynamics. Two independent models are constructed to represent the transducer behavior under normal and transverse impact forces. These models are built from the sampled measurements, by means of appropriate mathematical techniques for system identification. An autoregressive model polynomial contains information regarding natural frequencies and damping characteristics, and it is constructed by fitting the polynomial to the free response. A moving-average model polynomial represents the phase and magnitude of the transducer's free response, and it is developed by curve fitting spectral information. With these polynomials conforming what is called an ARMA model, the impact measurements are filtered so that the original signals are reduced to the "true" impact forces, by means of a deconvolutional process. The calculated impact forces are useful to infer information about the events that take place in the interval of projectile-transducer interaction.

Chapter 1

Introduction

1.1 Historical background

The study of impact phenomena can be traced back to the early efforts of applied mathematicians and physicists to represent it analytically. As in many other cases in the history of applied science, the study of colliding bodies depends heavily upon the availability of mathematical tools and general physical laws.

In the 18th century, when the field of applied mechanics emerged dramatically from its previous pre-scientific form, impact phenomena were modeled by algebraic equations of momentum and kinetic energy. The approach was to consider the bodies as rigid, point-mass entities. The main problem was to predict the overall impact effect, including the final velocities, by introducing concepts such as the coefficient of restitution.

Early in this century, the response of dynamic systems to impulsive forces was recognized as an important way of characterizing them. Incidentally, a problem of general interest consists of estimating the dynamic free behavior of a system, after initial conditions are applied as a result of an impact or impulsive load. Several analytical techniques were developed, but their application has been limited to simple models and

geometries.

In the last 50 years, major technological and mathematical advances have made possible the experimental and theoretical study of bodies and systems under impulsive dynamic forces. Experimental techniques include the use of digital equipment for data collection and processing, the introduction of several different kinds of transducers, and the extensive use of computers. Mathematical techniques for dealing with very complex high order systems have been developed, such as the finite element method (FEM), and the group of numerical techniques intended to model dynamic systems from records of input-output data, known as System Identification (SI).

1.2 Motivation for the study of impact processes

As in many other cases in engineering and science, the study and understanding of impact is relevant in our industrial societies because many technological processes and developments involve this kind of phenomenon. To mention only some applications of this field of knowledge:

(a) The design and construction of engineering structures intended to withstand stresses and deformations derived from impulsive forces require the ability to estimate their effects on the structure. Finite element models have been extensively used to simulate impact phenomena in spacecraft, aircraft and automotive components and structures [ref.11] and many others. Also, lumped parameter models have been proposed to explain the complex interactions and behavior of deformable bodies in collision [ref.6 and 8]. Some models are even intended to represent permanent deformation due to plastic behavior and fracture in the structures [references 3 and 6]. Special attention has been focused on the design

of vehicle structures capable of collapsing in a desired fashion so that the integrity of the occupant's space is guaranteed [ref 32].

(b) The planning and calculation of the amount of energy necessary to perform certain industrial operations and the effects of these processes on tools and machines have also been modeled by discretization and numerical procedures [ref.11].

The importance of understanding impact is not only practical, but also a theoretical aspect. Interestingly, the field of theoretical physics has borrowed the notion of "particle impact" in the construction of models for explaining complex processes. One of them, the so-called "chain reaction" paradigm, is a model of electrons and heavy-atoms represented as particles of different sizes in motion. Continuous collisions of electrons and heavy atoms make the latter release new electrons, and the process goes on and on. Another example is the model proposed for explaining the flow of free electrons when an electric current is present in a crystalline material. Again, the electrons are represented as particles in motion under the action of an electric field. Continuous collisions of atoms and free electrons in the crystalline material make the former vibrate, generating heat. There are other examples in the field of statistical thermodynamics as well.

1.3 The piezoelectric transducer apparatus

An important device in transducer technology, important in the experimental study of impact, is the piezoelectric force transducer. Even though the piezoelectric behavior of some crystals has been known for more than a century, it was not until the decade of 1940 when it began to have practical use in instrumentation. Before that time it was not practical to take advantage of the property of some crystals that exhibit electrical charges

under mechanical loads, since it requires very-high-input-impedance amplifiers.

Piezoelectric force transducers are preferred over several other alternatives in force instrumentation because of their advantages. Most force transducers have an elastic sensing element whose deformation is a measure of the acting force. For the system to have useful sensitivity, a rather large compliance is required, and consequently, large deformations will be present. But these large deformations are not desirable because they introduce geometric changes into the force path, which in turn cause measurement errors. For a piezoelectric force transducer the sensing and the transducing elements are the same one, so while there is no need to measure a deformation, which is much smaller than with other measuring systems, there is a need to amplify an electric charge, which is proportional to the applied force. An additional important consequence of the relatively high mechanical rigidity of piezoelectric transducers is that they have high natural frequencies, which make them appropriate for performing measurements of extremely fast events, such as impact forces and sudden accelerations.

Essentially, a typical piezoelectric multiaxis-force transducer consists of a stack of quartz discs and the corresponding electrodes assembled into a steel housing. Since the piezoelectric property is directional, each disc has been machined in a specific crystal axis orientation, so that a sensitive axis coincides with each of the three orthogonal components of the force to be measured. For the axial (vertical) component, the force is transmitted to the corresponding disc by means of compression, whereas for the remaining 2 transverse (horizontal) components, the forces are transmitted by friction and shear. When a force F acts upon the transducer, it is transmitted to each of the discs with the same

magnitude and direction. Then, each disc produces an electric charge proportional to the force component acting along the corresponding specific axis, and it is in turn amplified up to an useful level. For this purpose, appropriate high-impedance charge amplifiers and data sampling systems are used so that the information can be read by a computer and stored in its memory.

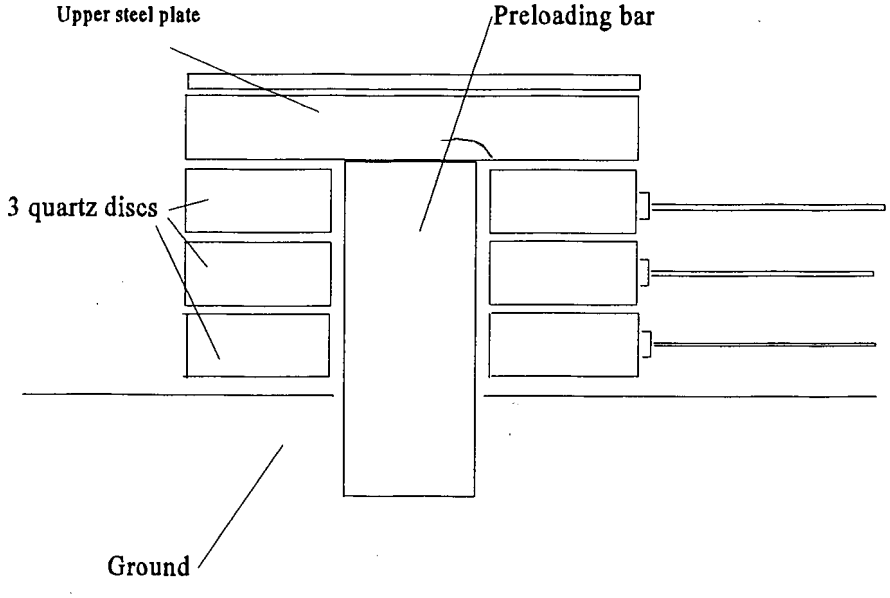

Figure 1.1 The piezoelectric transducer structure

Chapter 2

Impact force measurement with a piezoelectric transducer

2.1 Problem statement

The purpose of this work is to calculate the impact forces of a golf ball against a rigid barrier, from measurements taken with a piezoelectric transducer. The golf ball is projected at a high velocity by an air cannon and collides at a certain angle on the transducer surface, which plays the role of the rigid barrier. The impact forces can be represented by two orthogonal components, i.e. normal and transverse.

During the impact process, the energy transfer from the ball to the transducer is so intense that it produces vibrations of the transducer structure. As a result the electric output of the transducer does not correspond to the impact forces, includes dynamic forces internal to the transducer itself. The problem then consists of estimating the "true" impact forces, given sampled measurements of the total transducer dynamic signals..

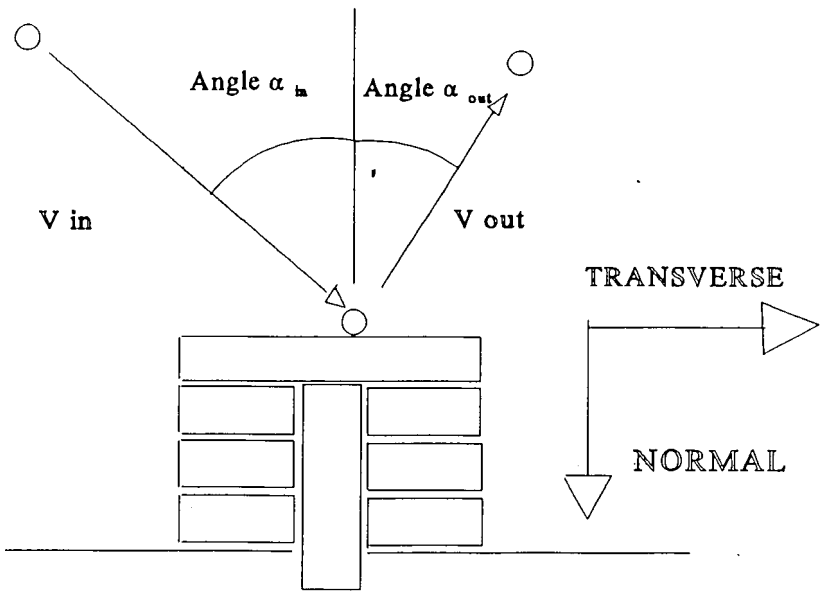

Figure 2.1 The projectile-piezoelectric transducer impact

2.2 Scope of this thesis

As pointed out before, since the transducer behaves as a dynamic system under the rapid application of impact forces, a logical approach is to build a model for the transducer consistent with these vibrations. It is important to notice that, since the impact phenomenon has a finite duration, the transducer vibrations are free or unforced in the interval following the impact. The idea is to build a dynamic model consequential to the measured dynamic behavior and, by means of an appropriate numerical procedure, to estimate the profiles of the unknown forces that generated the vibrations. Several different kinds of models have been used for representing structures under impact. They can be classified in two large groups, namely distributed parameter and lumped

parameter models. The transducer will be represented as two independent, discrete time, lumped parameter models. The two models will represent the phenomena in the transverse and normal orientations, relative to the transducer surface. These models are assumed to be independent since the transducer is designed to measure orthogonal forces independently.

In Chapter 3 the general structure for the model is established and several characteristics of the process, such as measurement noise and crosstalk, are introduced in the model. In Chapter 4, a numerical technique for estimating the order of the system from measurements of the free response is presented. The procedure is based on the concept of observability and identifiability and is intended to compensate for the effects of correlated noise embedded in the data. Chapter 5 is concerned with the first stage of the model identification procedure. Essentially, a model is fitted to the free response sequences by means of an iterative version of the least-squares technique. The identification of this model has to be iterative in order to compensate for the presence of correlated perturbations in our measurements due to crosstalk between different channels of the transducer. This first model contains information about natural frequencies and damping of the system. Then, Chapter 6 presents the second stage of the identification process: the model is completed taking into account the initial conditions of the system free response. A non-parametric technique is used in order to curve-fit the free-response discrete Fourier transform with two polynomials. A set of Markoff parameters is calculated from these polynomials, and this information is then used to complete the model for the transducer. Finally, the overall gain is calibrated using constants

provided by the manufacturer, in order to account for amplifier gains, so that the calculation of the impact forces yields appropriate units, such as Newtons or pounds. Once the model is available, the calculation of impact forces becomes a standard deconvolution (or filtering) problem. Chapter 7 contains the numerical results of the identification and deconvolution processes and presents the conclusions. Finally, Chapter 8 contains observations for future study of this problem.

Chapter 3

Setting up the model

3.1 Sampling the impact process measurements

As pointed out before, only the vibration measurements for transverse and normal phenomena are available, namely $x_N(t)$ and $x_T(t)$ respectively. The process is being sampled at intervals of T_s, and appropriate representations for the measurements are

$$\overline{x_N}(k) = \sum_{k=0}^{\infty} \delta(t-kT_s)\, x_N(kT_s) \qquad (3.1)$$

$$\overline{x_T}(k) = \sum_{k=0}^{\infty} \delta(t-kT_s)\, x_T(kT_s) \qquad (3.2)$$

Notice that the summations start at k=0, implying that the impact process begins there. The character δ represents the Kronecker-delta, and the overbar indicates the sampled function. The index k indicates the position of the samples in the sequence. Now, taking Laplace transform of equations (3.1) and (3.2), and recalling that the Laplace transform of the δ function is:

$$\mathcal{L}[\,\delta(t-a)\,] = e^{-a*s} \qquad (3.3)$$

we obtain from each of expressions (3.1) and (3.2):

$$F_N^* = \mathcal{L}\,[\overline{x_N}(k)\,] = \sum_{k=0}^{\infty} x_N(kT_s)\, e^{-S*k*T_s} \qquad (3.4)$$

and

$$F_T^* = \mathcal{L}[\overline{X_T}(k)] = \sum_{k=0}^{\infty} x_T(kT_s)\, e^{-S*k*T_s} \qquad (3.5)$$

and defining a new variable z in terms of the complex frequency s

$$Z \triangleq e^{S*k*T_s}$$

it is possible to rewrite equations (3.4) and (3.5) as follows

$$ZT(\overline{x_N}(k)) = \sum_{k=0}^{\infty} x_N(kT_s)\, z^{-k} \qquad (3.6)$$

$$ZT(\overline{x_T}(k)) = \sum_{k=0}^{\infty} x_T(kT_s)\, z^{-k} \qquad (3.7)$$

The last two equations are the conventional z-transforms (ZT) of the corresponding sampled signals at each channel. Notice that they are in the form of infinite Laurent series and that the coefficients of each power of the variable z are the ordered samples of the signals. The impact forces, namely $u_N(t)$ and $u_T(t)$, can also be treated in the same way, so that their z transforms also take the form of Laurent series

$$ZT[\overline{u_N}(k)] = \sum_{k=0}^{N_c} u_N(kT_s)\, z^{-k} \qquad (3.8)$$

$$ZT[\overline{u_T}(k)] = \sum_{k=0}^{N_c} u_T(kT_s)\, z^{-k} \qquad (3.9)$$

Notice that the z transforms of the impact forces have been truncated at the N_c position, since the time of contact projectile-transducer is finite and is supposed to consist of only $N_c + 1$ samples. In general, the number N_c is not a known quantity.

The purpose of this work is to reconstruct the N_c+1 coefficients of the impact forces by means of appropriate models.

3.2 The ARMA model for the transducer dynamics

By assumption, x_N and x_T are the outputs of independent linear systems. A linear system is characterized uniquely by its impulse response sequence

$$\overline{h}(k) = \sum_{k=0}^{\infty} \delta(t-kT_s)\, h(kT_s) \qquad (3.10)$$

or, in the z transform domain

$$H(z) = ZT(\overline{h}(k)) = \sum_{k=0}^{\infty} h(kT_s)\, z^{-k} \qquad (3.11)$$

Under rather general conditions, H(z) can be expressed also as a rational function, i.e., the quotient of two polynomials of order N in the variable z:

$$H(z) = \frac{\sum_{n=0}^{N} a_n z^{-n}}{1 + \sum_{n=1}^{N} b_n z^{-n}} = \frac{a_0+a_1 z^{-1}+\ldots+a_N z^{-N}}{1+b_1 z^{-1}+\ldots+b_N z^{-N}} \qquad (3.12)$$

and it is also called the transfer function. It represents the ratio of the output z-transform to the input z-transform:

$$H(z) = \frac{\sum_{k=0}^{\infty} x(kT_s)\, z^{-k}}{\sum_{k=0}^{N_c} u(kT_s)\, z^{-k}} \qquad (3.13)$$

Now, we make equations (3.13) and (3.12) equal, since they represent two different

expressions for the system transfer function. So, we have

$$\frac{a_0+a_1z^{-1}+a_2z^{-2}+\ldots+a_Nz^{-N}}{1+b_1z^{-1}+b_2z^{-2}+\ldots+b_Nz^{-N}} = \frac{\sum_{k=0}^{\infty} x(kT_s)\,z^{-k}}{\sum_{k=0}^{N_c} u(kT_s)\,z^{-k}} \qquad (3.14)$$

After developing the series and doing some algebraic manipulations we have

$$[a_0+a_1z^{-1}+\ldots+a_Nz^{-N}]*[u(0)+u(T_s)z^{-1}+u(2T_s)z^{-2}+\ldots]=$$

$$[1+b_1z^{-1}+\ldots+b_Nz^{-N}]*[u(0)+u(T_s)z^{-1}+u(2T_s)z^{-2}+\ldots] \qquad (3.15)$$

Expanding the products of the expressions in eq. (3.15) and equating the coefficients of like powers of z, it is possible to re-write an equivalent formula in the vector-matrix form. Notice that this expression is valid only for the case in which the number of values of u is less than or equal to Nc+1.

$$\begin{bmatrix} x(0) & x(T_s) & x(2T_s) & \cdots & x(NT_s) \\ x(T_s) & x(2T_s) & x(3T_s) & \cdots & x((N+1)T_s) \\ \vdots & \vdots & \vdots & \cdots & \vdots \\ x(jT_s) & x((j+1)T_s) & x((j+2)T_s) & \cdots & x((j+N)T_s) \end{bmatrix} \begin{bmatrix} b_N \\ b_{N-1} \\ \vdots \\ b_1 \\ 1 \end{bmatrix} =$$

$$\begin{bmatrix} u(0) & u(T_s) & u(2T_s) & \cdots & u(NT_s) \\ u(T_s) & u(2T_s) & u(3T_s) & \cdots & u((N+1)T_s) \\ \vdots & \vdots & \vdots & \vdots & \vdots \\ u(jT_s) & u((j+1)T_s) & \cdots & \cdots & u((j+N)T_s) \end{bmatrix} \begin{bmatrix} a_N \\ \\ \vdots \\ a_0 \end{bmatrix} \qquad (3.16)$$

Equation (3.16) represents the input-output relationship of a dynamic system. This expression is useful for calculating the input sequence u(kTs), k=0,1,... as long as the output values x(kTs) and the model parameters (a_i and b_i) are available. In the problem at hand this is not the case. The output x(kTs) is available but under noisy conditions, as we shall see, and the model parameters are unknown. Even the system order N is unknown. The process of estimating the model parameters, essential to the calculation of the impact force coefficients, defines the nature of the problem; in other words, this is an identification problem.

A particularly useful recurrence expression can be written from equation (3.16) by observing the regularity in the indexes at every row. This expression, often called "autorregressive-moving average" (ARMA), takes the following structure:

$$\bar{x}(k)+\bar{x}(k-1)\,b_1+\cdots+\bar{x}(k-N)\,b_N=\bar{u}(k)\,a_0+\cdots+\bar{u}(k-N)\,a_N \qquad (3.17)$$

We can isolate the value x_k and obtain a prediction equation for it:

$$\bar{x}(k)=\bar{u}(k)\,a_0+\cdots+\bar{u}(k-N)\,a_N-\bar{x}(k-1)\,b_1-\cdots-\bar{x}(k-N)\,b_N \qquad (3.18)$$

The autorregresive part is defined by the prediction of the new x_k by the contribution of the preceding values in the sequence, whereas the moving-average portion of the model consists of the contribution of the weighted average of an exogenous sequence u.

3.3 Noise in the measurements

Noise is an omnipresent phenomenon in real physical processes. The piezoelectric

transducer and the corresponding electronic instrumentation present two different kinds of noise sources: those of deterministic nature, and those of random type.

a) Random noise: this kind of perturbation is composed of all phenomena that are difficult to predict . Quantization is probably the most important component, and it is inherent to the very essence of sampled digital systems. It consists of the error introduced by the measuring device when each measurement is "rounded" or "truncated" as it is converted to a binary sequence of ones and zeros.

b) Deterministic noise: this kind of exogenous interference in our measurements is due to the fact that, even though each channel is supposed to be independent, we obtain residual effects due to the other channels. This phenomenon is commonly called crosstalk and it can be readily detected in a spectral plot.

To be more specific in the mathematical representation of the noise effect, consider the following expressions :

$$\overline{x_N^*}(k) = H_N\overline{u_N} + H_{NT}H_T\overline{u_T} + \epsilon_N \qquad (3.19\text{-}a)$$

$$\overline{x_T^*}(k) = H_T\overline{u_T} + H_{TN}H_N\overline{u_N} + \epsilon_T \qquad (3.19\text{-}b)$$

This last representation now includes additive noise in the measurement and also takes into account the cross-talk noise in the form of additional transfer functions from one output to the other represented with double subindex. A block-diagram representing these equations appears in fig.3.1. The inclusion of transfer functions from each output to the other implies the assumption that crosstalk is only an interference of each channel output on the other. The position of crosstalk perturbations in the frequency

domain is such that we can actually moderate its effect by applying conventional low-pass digital filters to the information. Such operation will enhance the accuracy of the identification process by minimizing the presence of noise, particularly of crosstalk, so that the estimation error will decrease, and then it will be possible to assume a single source of noise in the measurement. The following equations represent the system after applying low pass filtering:

$$\overline{x_N^*} = \overline{x_N} + \overline{e_N^*} = H_N\overline{u_N} + \overline{e_N^*} \qquad (3.20\text{-}a)$$

$$\overline{x_T^*} = \overline{x_N} + \overline{e_T^*} = H_T\overline{u_T} + \overline{e_T^*} \qquad (3.20\text{-}b)$$

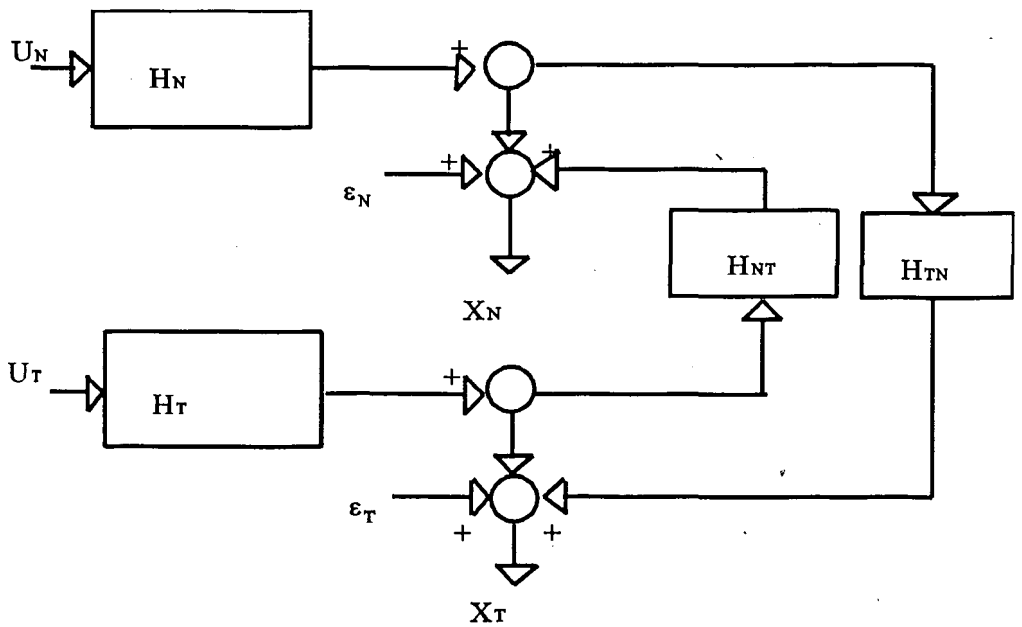

Figure 3.1 Block diagram for the compiete transducer model

Comparing expressions (3.18) and (3.19), we see that after the low pass filter process is applied the cross terms H_{TN} and H_{NT} disappear, and there remains only an additive

noise in the output. Later on we shall see that it is convenient to get rid of the crosstalk before beginning the identification process, since otherwise its deterministic nature would make our calculations identify crosstalk as part of the true modes of vibration, which would be certainly incorrect. (see figure 3.2).

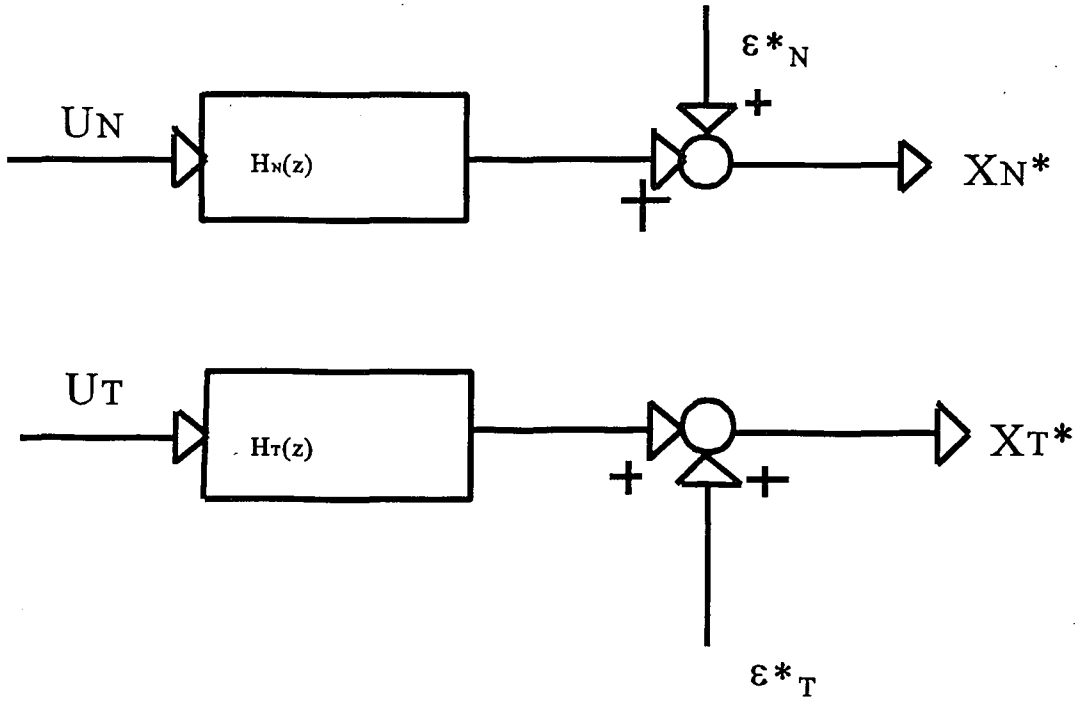

Figure 3.2 Two independent models for normal and transverse phenomena.

3.4 Outline of the identification procedure

The ARMA model parameters $\{a_i, b_i\}$ are essential for calculating the input sequence $\{ u_i \}$, as can be seen in equation (3.16). Since appropriate models for

each channel of the piezoelectric transducer are not available *a priori*, the first task is to solve the identification problem, that is to say, find a set of appropriate model parameters so that the corresponding models are self-consistent, in the sense that they represent the transducer dynamics under impact. Notice that the measurements of the transducer vibrations can be separated into two regimes: forced and autonomous. The first one corresponds to the interval of interaction between the projectile and the transducer, for which the input force is different from zero, whereas the latter comprises the subsequent free vibration in the interval following the projectile-transducer contact and for which the input force is zero. The measurement samples of the free vibration interval correspond to the foreshortened impulse response sequence. We say foreshortened because the first values are embedded in the forced sequence measurements, and thus they are not readily available.

The first step in the identification procedure consists of the estimation of the system order {N} for transverse and normal phenomena. This is done by applying a rank test to segments of the impulse response sequence (also called "Markoff parameters" in the literature of time-series analysis), arranged in the form of Hankel matrices. These tests are developed from the concepts of observability and identifiability of dynamical systems, and they are applied extensively in order to increase the level of significance in the matrix singularity so that we account for the presence of correlated noise, which is residual from crosstalk perturbations. The supporting theory is presented in Chapter 4.

Once the system order is known, an ARx (autorregressive exogenous model) is fit to the free response sequence. The approach is based on least squares theory, and it will be

applied in an iterative fashion in order to progressively remove the bias in the estimation due to the fact that the noise is correlated. The AR model is a polynomial containing information about hidden periodicities in the autonomous sequence. In other words, the ARx identification will yield estimations for the system's poles. The algorithm is adapted from a method known as "generalized least squares" and is presented in Chapter 5.The next step in the identification process consists of estimating the MA polynomial. It will be shown that the AR and MA polynomials are related to each other by a Toeplitz-like matrix and a vector built from the first N+1 Markoff parameters. Since the AR polynomial is already known from previous computations, there is a need to estimate these first Markoff parameters, which are not available since they are embedded in the first N+1 measurements of the forced process (the interval of projectile-transducer interaction). A method borrowed from aerospace-structure modal identification is used in order to curvefit the discrete Fourier transform (DFT) of the impulse response, and then the desired Markoff parameters can be easily obtained from the mathematical approximation of the free response DFT. For some cases, the spectral information in the impulse response sequence DFT is overlapped by that of the forcing function, so that it is not possible to curve-fit its DFT information. In this case, a fictitious impulse response will be introduced starting at an arbitrary location, a MA model will be calculated for this case, and then the impulse response sequence will be propagated backwards in time so that we will have the desired initial set of Markoff parameters. The sustaining theory is included in Chapter 6.

Finally, the complete ARMA model will be calibrated by adjusting the low frequency

gain, using constants provided by the manufacturer, so that the input force can be calculated in standard force units, such as Newtons. A justification of this process will be given also in Chapter 6. With the model available, the calculation of impact forces is done by a deconvolutional (or filtering) process.

Chapter 4

Finding the system order

The purpose of this chapter is to develop a methodology appropriate for estimating the size of the ARMA model for the transducer under an impact process .This size is the order of the polynomials in the model. Since a considerable proportion of our measurements corresponds to the system's free response, it makes sense to use these values for such estimation. As we shall see, two important classical concepts, namely observability and identifiability, are the backbone of our method.

4.1 The concept of observability for a dynamical system

Consider the general unforced dynamical system, described by these equations:

$$\overline{x}(k+1) = \Phi\overline{x}(k) \qquad (4.1\text{-}a)$$

$$\overline{h}(k) = C\overline{x}(k) \qquad (4.1\text{-}b)$$

where Φ is the state-transition matrix, and the over bar indicates that the expression is that of a discrete-time system. Here the sequence x is the set of states, and the sequence h is called the measurement vector of the impulse-response sequence.

Observability is the property of a dynamical system that permits calculation of the states from the measurements {h} only. We can write the following relationships

$$\begin{aligned} \bar{x}(1) &= \phi\bar{x}(0) & \bar{h}(0) &= C\bar{x}(0) \\ \bar{x}(2) &= \phi^2\bar{x}(0) & \bar{h}(1) &= C\phi\bar{x}(0) \\ &\vdots & &\vdots \\ \bar{x}(p-1) &= \phi^{p-1}\bar{x}(0) & \bar{h}(p-1) &= C\phi^{p-1}\bar{x}(0) \end{aligned} \qquad (4.2)$$

Equations (4.2) are the successive application of the relations defined in equations(4.1), so that we can see the effect of the initial condition x(0) on each one of the following intervals. Now, in the vector-matrix form we have

$$\begin{bmatrix} \bar{h}(0) \\ \bar{h}(1) \\ \bar{h}(2) \\ \vdots \\ \bar{h}(n-1) \end{bmatrix} = \begin{bmatrix} C \\ C\phi \\ C\phi^2 \\ \vdots \\ C\phi^{n-1} \end{bmatrix} \bar{x}(0) = R\bar{x}(0) \qquad (4.3)$$

Since our objective is to determine the initial state x(0) uniquely, then the matrix R, also called the observability matrix, must be non singular. Observe the structure of the matrix R:

$$R = \begin{bmatrix} C \\ C\phi \\ C\phi^2 \\ \vdots \\ C\phi^{n-1} \end{bmatrix}$$

Then the condition for observability is that R be full rank, or

rank(R) = n

If this is true, then the couple $\{\phi,C\}$ is called an observable pair. Notice that n is the system order.

4.2 The identifiability condition for an unforced system

Now that we know the inherent condition without which it is impossible to calculate the states from the measurements only, we can also find the required condition for system parameter determination given the states. In other words, we ask: under what conditions is it possible to estimate the entire set of system parameters, given the entire set of state samples. Notice that the system parameters for an unforced system are nothing but the values of the state transition matrix ϕ. Also notice that it is assumed in the very statement of the problem that all the states are available, which turns out to imply observability. In order to derive a condition for complete parameter identification, we write a sequence representing the free dynamics

$$\begin{aligned}
\bar{x}(1) &= \phi\bar{x}(0) \\
\bar{x}(2) &= \phi\bar{x}(1) = \phi^2\bar{x}(0) \\
\bar{x}(3) &= \phi\bar{x}(2) = \phi^3\bar{x}(0) \\
&\vdots \\
\bar{x}(n) &= \phi\bar{x}(n-1) = \phi^n\bar{x}(0)
\end{aligned} \tag{4.8}$$

Since by assumption all the states can be observed, it is possible to set up a matrix in the following fashion, after n sampling periods

$$\left[\, \bar{x}(1), \ \cdots \ \bar{x}(n-1) \right] = \left[\phi\bar{x}(0), \ \phi\bar{x}(1), \ \cdots \ \phi\bar{x}(n-1) \right]$$

$$= \phi \left[\, \bar{x}(0), \ \bar{x}(1), \ \cdots \ \bar{x}(n-1) \right] \tag{4.9}$$

For the parameters in ϕ to be uniquely defined, the following condition has to be true

$$\text{rank}(M) = n$$

where

$$M = \left[\bar{x}(0),\ \bar{x}(1),\ \cdots\ \bar{x}(n-1) \right] \qquad (4.10)$$

The matrix M is often called an n-identifiability matrix in the scientific literature (see Lee 1969). If rank(M)=n, then we say that the system is n-identifiable.

4.3 Order determination from samples of the impulse response

From sections 4.1 and 4.2 we can see that, if an unforced system is observable and n-identifiable, meaning that the matrices R and M have full rank, then it is possible to estimate the system parameters (values of the state transition matrix components) from the output measurements only, and these parameters will be unique. Now suppose that we have n measurements of an unforced system's free dynamics:

$$\Pi(1,n) \triangleq \begin{bmatrix} \bar{h}(1) \\ \bar{h}(2) \\ \vdots \\ \bar{h}(n) \end{bmatrix} \qquad (4.11\text{-}a)$$

$$\Pi(q,q+n-1) \triangleq \begin{bmatrix} \bar{h}(q) \\ \bar{h}(q+1) \\ \vdots \\ \bar{h}(q+n-1) \end{bmatrix} \qquad (4.11\text{-}b)$$

Now recall the following relationships

$$\overline{h}(i) = C\overline{x}(i)$$
$$\overline{x}(i) = \phi^{i-1}\overline{x}(0)$$

then, the generalized measurement matrix $\Pi(q,q+n)$ may be written

$$\Pi(q, q+n-1) = \begin{bmatrix} \overline{h}(q) \\ \overline{h}(q+1) \\ \vdots \\ \overline{h}(q+n-1) \end{bmatrix} = \begin{bmatrix} C\phi^{q}\overline{x}(0) \\ C\phi^{q+1}\overline{x}(0) \\ \vdots \\ C\phi^{q+n-1}\overline{x}(0) \end{bmatrix}$$

$$= \begin{bmatrix} C\phi^{q} \\ C\phi^{q+1} \\ C\phi^{q+2} \\ \vdots \\ C\phi^{q+n-1} \end{bmatrix} \overline{x}(0) = \begin{bmatrix} C \\ C\phi \\ C\phi^{2} \\ \vdots \\ C\phi^{n-1} \end{bmatrix} \phi^{q}\overline{x}(0) = R\phi^{q}\overline{x}(0) \qquad (4.12)$$

Now, we define a matrix comprising free-response information, as follows

$$\psi(1,2n-1) \triangleq \left[\begin{array}{c|c|c|c} & & & \\ \Pi(1,n) & \Pi(2,n+1) & \cdots & \Pi(n,2n-1) \\ & & & \end{array}\right] =$$

$$= \begin{bmatrix} \overline{h}(1) & \overline{h}(2) & \cdots & \overline{h}(n) \\ \overline{h}(2) & \overline{h}(3) & \cdots & \cdots \\ \vdots & \vdots & \vdots & \vdots \\ \overline{h}(n) & \overline{h}(n+1) & \cdots & \overline{h}(2n-1) \end{bmatrix} \qquad (4.13)$$

Matrix Ψ , defined as in equation (4.13), has a very particular structure. It is a square matrix formed with consecutive segments of the impulse response sequence {hi},and these consecutive segments are the matrices Π defined in equation (4.12). It is usually called

the Hankel matrix, and it is ubiquitous in the study and research of linear sampled systems.Now consider a factorization performed on the Hankel matrix of equation (4.13)

$$\psi(1,2n-1)=\left[\begin{array}{c|c|c|c} C\phi(\phi\overline{x_0}) & C(\phi^2\overline{x_0}) & C(\phi^3\overline{x_0}) & \cdots \\ C\phi(*\overline{x_0}) & C\phi(\phi^2\overline{x_0}) & C\phi(\phi^3\overline{x_0}) & \cdots \\ \vdots & \vdots & \cdots & \cdots \\ C\phi^{n-1}(\phi\overline{x_0}) & C\phi^{n-1}(\phi^2\overline{x_0}) & \cdots & \cdots \end{array}\right] \qquad (4.14)$$

Matrix Ψ in equation (4.14) is partitioned in such a way that each column still represents one segment of the impulse response sequence, as defined by the vector Π in equation (4.12). It can be seen that each column in the matrix Ψ can be expressed as the product of the observability matrix R and something else. This is strongly suggested by the particular disposition of the parenthesis in each term of matrix Ψ as it appears in eq. (4.14). Hence, the following decomposition permits the explicit expression of the observability matrix R as one factor in the following product:

$$\Psi(1,2n-1) = \begin{bmatrix} C \\ C\phi \\ \vdots \\ C\phi^{n-1} \end{bmatrix} \left[\phi\overline{x_0} \mid \phi^2\overline{x_0} \mid \cdots \mid \phi^n\overline{x_0}\right] =$$

$$= \begin{bmatrix} C \\ \vdots \\ C\phi^{n-2} \\ C\phi^{n-1} \end{bmatrix} \phi\left[\overline{x_0} \mid \phi\overline{x_0} \mid \cdots \mid \phi^{n-1}\overline{x_0}\right] \qquad (4.15)$$

Now it is possible to easily recognize that the right-hand factor in equation (4.15) is the n-identifiability matrix, so that the complete decomposition for the Hankel matrix is

$$\psi(1,2n-1) = R\phi B \qquad (4.16)$$

The identity in equation (4.16) permits us to find an essential characteristic of the impulse response sequence. If we assume that a certain dynamical system is observable and n-identifiable, then matrices R and N are nonsingular. Also, we know that a property of physical systems is that the state transition matrix ϕ is nonsingular. Under such circumstance we conclude that the Hankel matrix Ψ, comprising elements of the impulse response sequence of a system, is nonsingular as well.

In this spirit it is feasible to estimate the system order of an unforced system by evaluating the ranks of Hankel matrices constructed with segments of the impulse response sequence. In general, it holds that

$$rank(\ \Psi(q,p+q-1)\ ) = n$$

as long as the following statement is true:

$$p \geq \frac{(n-1)}{2}$$

Alternatively, we can evaluate the determinants of these Hankel matrices for each p= 2, 3,... and the system order will correspond to that value of p for which this statement holds

$$\det(\psi(q,p+q-1)) = 0 \qquad (4.17)$$

This method works for deterministic systems, i.e., those for which the measurements are noiseless. In practice, these determinants will not vanish identically because of noise

contained in the data. Hence, some criterion must be introduced in order to increase the level of significance. Our approach will be to calculate the average value of the determinants of $\Psi(q,p+q-1)$ for each p, always processing the same set of measurements, and plot the ratio J_p against p_n, where

$$J_p \triangleq \frac{|average\ value\ of\ \det(\psi(q,p_k+q-1))|}{|average\ value\ of\ \det(\psi(q,p_{k+1}+q-1))|} \qquad (4.18)$$

where $p_k = 1,2,3,4,\ldots$, and $p_{k+1}=p_k+1$. From this plot the order n is obtained as the integer number p_k for which J_p is a maximum. A complete justification of this procedure is rather complex and can be found in [26]. Essentially, the determinant of each Hankel matrix built up with noisy measurements is a nonlinear multivariable function of each element in a sequence of noise samples which form a random variable series. Therefore, the determinant is a random variable itself. If we assume that the noise to signal ratio is small, we can see that the average value of the determinants will converge to the deterministic determinant as long as a sufficiently large amount of information is processed (law of large numbers). These last statements are not a formal argument, but rather an explanation of why the method works.

Chapter 5

Finding periodicities in the transducer vibrations

5.1 The autoregressive law for the transducer free dynamics

Once the system order has been estimated following the algorithm presented in Chapter 4, the next step consists of estimating the parameters in the model. It will be accomplished in principle by constructing the denominator polynomial that defines the autoregressive nature of the transducer's free dynamics after impact. Consider equations (3.20) in a generic form

$$\overline{x^*}(k) = \bar{x}(k) + \epsilon^*(k) = H(z)\,\bar{u}(k) + \epsilon^*(k) \qquad (5.1)$$

Recall that the term $\{\epsilon^*\}$ represents the additive noise once the signal has been processed by an appropriate low-pass filter intended to decrease the presence of crosstalk. Recall the basic ARMA relationship in our model

$$(1 + \sum_{i=1}^{N} b_i z^{-i})\,\bar{x}(k) = (\sum_{i=0}^{N} a_i z^{-i})\,\bar{u}(k) \qquad (5.2)$$

Now, combining these last expressions, it is possible to obtain a new one in terms of noisy measurements only

$$(1 + \sum_{i=1}^{N} b_i z^{-i})\,(\overline{x^*}(k) - e^*(k)) = (\sum_{i=0}^{N} a_i z^{-i})\,\overline{u}(k) \quad (5.3)$$

In order to incorporate free vibration measurements, we set the input to be zero, and then an ARx model for the transducer is obtained for the interval after impact. If we define a fictitious noise v*(k) as follows

$$v^*(k) \triangleq (1 + \sum_{i=1}^{N} b_i z^{-i})\,e^*(k) \quad (5.4)$$

Then, we have

$$\overline{x^*}(k) = e^*(k) + \sum_{i=1}^{N} b_i e^*(k-i) - \sum_{i=1}^{N} b_i \overline{x^*}(k-i) \quad (5.5)$$

or, after introducing the definition of v*(k)

$$\overline{x^*}(k) = v^*(k) - \sum_{i=1}^{N} b_i \overline{x^*}(k-i) \quad (5.6)$$

If formula (5.6) is expanded, the resulting expressions may be written in vector matrix form. This following structure will be very useful for identification purposes

$$\begin{bmatrix} \overline{x^*}(k) \\ \overline{x^*}(k+1) \\ \overline{x^*}(k+2) \\ \vdots \\ \overline{x^*}(k+p) \end{bmatrix} = -\begin{bmatrix} \overline{x^*}(k-N) & \overline{x^*}(k-N+1) & \cdots & \overline{x^*}(k-1) \\ \overline{x^*}(k-N+1) & \overline{x^*}(k-N+2) & \cdots & \overline{x^*}(k) \\ \overline{x^*}(k-N+2) & \overline{x^*}(k-N+3) & \cdots & \overline{x^*}(k+1) \\ \vdots & \vdots & \vdots & \vdots \\ \overline{x^*}(k+p-N) & \cdots & \cdots & \cdots \end{bmatrix} \begin{bmatrix} b_N \\ b_{N-1} \\ \vdots \\ b_2 \\ b_1 \end{bmatrix} + \begin{bmatrix} v^*(k) \\ v^*(k+1) \\ \\ \vdots \\ \end{bmatrix} \quad (5.7)$$

We can define each element in this last expression in order to have a short hand version of it

$$\overline{X^*} + (A^*)\theta + V^* \qquad (5.8)$$

where each term is defined as

$\overline{X^*} \triangleq$ *vector of measurements*

$A^* \triangleq$ *records of past information*

$\theta \triangleq$ *vectorof AR parameters*

$V^* \triangleq$ *vector of innovations*

We can think of the innovations sequence as the input to the AR process that originates the noise ϵ^*, often called the residual.

5.2 A preliminary AR estimation by ordinary least squares

Once an appropriate structure for identification, such as equation (5.7), has been established, a preliminary parameter estimation is feasible by means of the ordinary least squares technique. Consider equation (5.8). Notice that if the innovations sequence V* were zero, then p+1 measurements would be sufficient for estimating the vector θ, so that the matrix A* would be square, and its inversion would provide the desired estimation. Under the effects of noisy measurements, a criterion should be determined so that the parameter estimates are optimal under such a policy. Let θ_{opt} be the best estimation under a minimum error-square criterion. In contrast, the "true" parameters will be called θ_{true}. Then, the difference between the estimate and the actual value is:

$$\Delta\theta = \theta_{true} - \theta_{estimate} \qquad (5.9)$$

In an analogous fashion, there is a difference between the output of the model

with estimated parameters, and the output of the real model

$$\Delta\overline{X^*} = \overline{X^*_{true}} - \overline{X^*_{estimate}} \qquad (5.1$$

also, the output of the model with estimated parameters is given by

$$\overline{X^*_{estimate}} = (A^*)\theta_{estimate} \qquad (5.11)$$

therefore, combining expressions (5.11) and (5.10) we have

$$\Delta\overline{X^*} = \overline{X^*} - (A^*)\theta_{estimate} \qquad (5.12)$$

Now, the criterion of minimization, namely minimum square error, is set to be

$$E^2 \triangleq (\Delta\overline{X^*})^T(\Delta\overline{X^*}) \qquad (5.13)$$

In this last expression the superscript T is the transpose operator, and E^2 is the function error square. The optimal estimate θ_{opt} will be the parameter vector which minimizes (5.23). In order to perform this minimization the function error square is written in terms of θ_{est},:

$$E^2 = (\overline{X^*} - (A^*)\theta_{estimate})^T(\overline{X^*} - (A^*)\theta_{estimate}) \qquad (5.14)$$

For the value of $\theta_{estimate}$ to be optimal, the derivative of E^2 with respect to $\theta_{estimate}$ has to be equal to zero. For that purpose we expand the expression for the error square and then the corresponding derivative is calculated, following the rules of differentiation for vectors and matrices:

$$E^2 = \overline{X^{*T}X^*} - \overline{X^{*T}}A^*\theta_{est} - (A^*\theta_{est})^T\overline{X^{*T}} + (A^*\theta_{est})^TA^*\theta_{est} \qquad (5.15)$$

differentiating and equating to zero

$$\frac{d(E^2)}{d\,\theta_{est}} = -\overline{X^{*T}}A^{*} - (A^{*T}\overline{X^{*}})^{T} + 2\theta_{est}^{T}A^{*T}A^{*} = 0 \qquad (5.16)$$

And therefore, under such condition θ_{est} becomes θ_{opt}, so that

$$\theta_{opt} = (A^{*T}A^{*})^{-1}A^{*T}\overline{X^{*}} \qquad (5.17)$$

Notice that the expression for θ_{opt} involves the pseudoinverse of the matrix of past records, A*. This important result has been used in the field of system identification for more than 30 years. It is well known that this estimate is biased ,i.e., the expected value for the error is different from zero, if the noise is correlated. This is the case in our particular application, since one source of noise is crosstalk, and there is a need for improvement of this first estimation, in order to decrease the adverse effect of the correlated disturbance.

5.3 Improving the AR parameter estimates by iteration

It has been shown by several researchers,e.g., Eyckhoff and Åstrom, that if the noise affecting our measurements is correlated, then the parameter estimates given by equation (5.17) will be biased in the sense that the expected value of the error will not be zero. In that case it is still possible to improve the estimation by including a model of the noise process in the identification method. In general, if a noise sequence is correlated, then it can be expressed as the output of an AR process for which the input is a Gaussian, finite variance random variable (see, for example, Hsia or Clarke). To be more specific, consider the following structure for the noise model

$$e(k) = \left(1 + \sum_{i=1}^{r} c_i z^{-i} \right) v^*(k) \qquad (5.18)$$

Here, e(k) is a white, finite variance random variable, and the values v*(k) are called innovations, because for each value of k, it provides the only "new" external influence that the sequence ϵ*(k) has. A block-diagram presenting the complete model can be found in figure (5.1). This structure can be understood from another point of view. In a particular sense we are introducing a "prewhitening" filter, which is intended to convert the correlated sequence v*(k) into a Gaussian one, e(k). The block between signals e(k) and v*(k) is conventionally called an innovations filter, and its inverse is a whitening filter, because, if applied to the sequence v*(k), it would become a white noise sequence. Returning to equation (5.18), it can be seen that the parameters c_i are not known. Even the order r is not a known quantity. We can develop the preceding expression in a way analogous to that of equation (5.7). We have

$$\begin{bmatrix} v^*(k) \\ v^*(k+1) \\ v^*(k+2) \\ \\ \vdots \end{bmatrix} + \begin{bmatrix} v^*(k-r) & v^*(k-r+1) & \cdots & v^*(k-1) \\ v^*(k-r+1) & v^*(k-r+2) & \cdots & v^*(k) \\ v^*(k-r+2) & \cdots & \cdots & v^*(k+1) \\ v^*(k-r+3) & \cdots & \cdots & v^*(k+2) \\ \vdots & \vdots & \vdots & \vdots \end{bmatrix} \begin{bmatrix} c_r \\ c_{r-1} \\ \\ \vdots \\ c_1 \end{bmatrix} = \begin{bmatrix} e(k) \\ e(k+1) \\ e(k+2) \\ \\ \vdots \end{bmatrix} \qquad (5.19)$$

or, by defining new matrices we can abbreviate the equation

$$V^* = (B^*)(\theta_c) + e \qquad (5.20)$$

Notice the following relationship, readily obtained from equations (5.19) and (5.4)

$$e(k) = (1 + \sum_{i=1}^{r} c_i z^{-i}) \; (1 + \sum_{i=1}^{N} b_i z^{-i}) \epsilon^*(k) \qquad (5.21)$$

or, in shorthand notation, by defining again a new matrix, we have

$$e(k) = \Omega(z) \epsilon(k) \qquad (5.22)$$

The polynomial $\Omega(z)$, consisting of r+p+1 terms, is a prewhitening filter acting upon the residual sequence ϵ^*. By processing our signal with the action of this filter, the exogenous noise will become white, and then it will be possible to apply the conventional formula for least-square-error estimation, and thus obtain an unbiased estimate. The problem now consists of the estimation of parameters c_i. It is evident that the process of estimating the parameters c_i is entirely analogous to that of finding the values b_i. Consider equation (5.4) again. Premultiplying the last expression by the prewhitening filter, we obtain the following expression

$$(1 + \sum_{i=1}^{p} c_i z^{-i}) \; (1 + \sum_{i=1}^{N} b_i z^{-i}) \overline{x^*}(k) = (1 + \sum_{i=1}^{p} c_i z^{-i}) \; v^*(k) \qquad (5.23)$$

If we define the filtered signal in the left hand of equation (5.23) as

$$\overline{x^{**}}(k) = (1 + \sum_{i=1}^{r} c_i z^{-i}) \overline{x^*}(k) \qquad (5.24)$$

then, after substituting this new defined signal into equation (5.22), and noticing that it is equal to e(k), we have

$$(1 + \sum_{i=1}^{N} b_i z^{-i}) \overline{x^{**}}(k) = e(k) \qquad (5.25)$$

This last relationship can be expanded in the customary fashion, and expressed in the vector-matrix form

$$\overline{X^{**}} + A^{**}\theta + e \qquad (5.26)$$

It can be seen that the structure of equation (5.26) is entirely analogous to that of equation (5.8). By means of an appropriate prewhitening process, it has been possible to convert the system to one driven by a purely white, Gaussian noise. Then, the ordinary equation for least-squares estimation can be applied. The idea behind this formulation is really to build models for the noise and the system alternately, based upon appropriate information, so that the bias in the estimation is gradually removed.

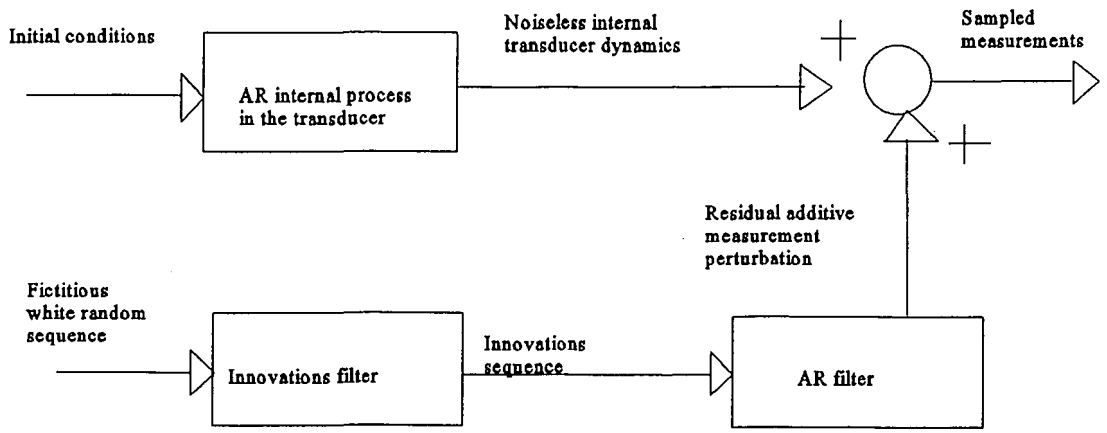

Figure 5.1 Block diagram for the AR prewhitening filter implementation

The algorithm can be structured in the following steps:

1 The initial step consists of calculating an initial estimate by means of the least squares formula. This is the zero-th iteration. Notice that the matrix of past information A* remains the same for all steps

$$\theta^{0}_{opt} = (A^{*T}A^{*})^{-1}A^{*}\overline{X^{*}}$$

2 Then, we calculate the innovations sequence by filtering the measurements in this way:

$$V^* = (1 + \sum_{i=1}^{N} b_i z^{-i})\,\overline{x^*}(k)$$

3 Next, the matrix B is constructed with the innovations, and a least-squares estimate is constructed for the noise process

$$\theta^j_{noise} = (B^T B)^{-1} B V^*$$

4 Now, we filter the measurement signal using the parameters of the noise process as a prewhitening filter

$$\overline{x^{**}}(k) = (1 + \sum_{i=1}^{r} c_i z^{-i})\,\overline{x^*}(k)$$

5 And then, evaluate θ_{opt} by using again the ordinary least-squares formula with the appropriate components

$$\theta^j_{opt} = (A^{**T} A^{**})^{-1} A^{**} \overline{X^{**}}$$

And, in order to measure the performance of our estimation, we calculate the error square, which is supposed to decrease and converge to a minimum as the estimation process goes on

$$E_j^2 = (\overline{X^*} - (A^*)\,\theta^j_{opt})^T (\overline{X^*} - (A^*)\,\theta^j_{opt})$$

6.- Repeat steps 2 through 5 until the condition for convergence is met, namely

$$E^2_{j+1} - E^2_j = 0$$

Chapter 6

Reconstruction of phase and amplitude for the transducer dynamics

This chapter is concerned about the development of a methodology appropriate for estimating the remaining unknown parameters in the ARMA model, i.e., the coefficients in the numerator, and the overall gain . This methodology is based on a technique borrowed from the field of aerospace structure identification, and has proven useful for modeling vibrating structures with hundreds of modes.

6.1 Relationship between AR and MA parameters

In Chapter 5, a procedure for the estimation of the MA parameters from the transducer's free dynamics was presented. It is relevant now to determine a relationship between the MA and the AR parameters of the model, so that the values of the latter can be incorporated into the calculation of the components of the former. Recall from equation (3.11) that the transfer function for a dynamic system can be written in terms of a Laurent series for which the coefficients are samples of the impulse response function

$$H(z) = \sum_{k=0}^{\infty} \overline{h}(k)\, z^{-k} \qquad (6.1)$$

In general, this last representation is extended to infinity, since a transducer is usually

a very lightly damped system, so that the free vibrations take a considerable number of samples to die out completely. Equating expression (6.1) to the ARMA structure

$$\sum_{k=0}^{\infty} \bar{h}(k)\, z^{-k} = \frac{\sum_{n=0}^{N} a_n z^{-n}}{1 + \sum_{n=1}^{N} b_n z^{-n}} \qquad (6.2)$$

At this point it is possible to cross-multiply and expand the expression, and after collecting terms of like powers of z we have

$$a_0 + a_1 z^{-1} + \ldots + a_{Nz}^{-N} = \bar{h}(0) + (\bar{h}(1) + b_1 \bar{h}(0))\, z^{-1} +$$

$$\ldots + (\bar{h}(N) + \sum_{i=1}^{N} b_i \bar{h}(N-i))\, z^{-N} + \ldots) \qquad (6.3)$$

We can now equate coefficients of the same power of z, and write it in the vector-matrix form. Only N+1 equations will be retained, since they represent completely the desired relationship between the AR and the MA parameters

$$\begin{bmatrix} a_0 \\ a_1 \\ a_2 \\ \vdots \\ a_N \end{bmatrix} = \begin{bmatrix} 1 & 0 & 0 & 0 & \ldots & 0 \\ b_1 & 1 & 0 & 0 & \ldots & 0 \\ b_2 & b_1 & 1 & 0 & \ldots & 0 \\ \vdots & \vdots & \vdots & \vdots & \vdots & \vdots \\ b_4 & b_3 & b_2 & b_1 & \ldots & 0 \end{bmatrix} \begin{bmatrix} \bar{h}(0) \\ \bar{h}(1) \\ \bar{h}(2) \\ \vdots \\ \bar{h}(N) \end{bmatrix} \qquad (6.4)$$

Then, it can be seen that the relationship between the AR and the MA parameters involves a Toeplitz-like matrix constructed with the {bi} values and a vector of the first N+1 values on the impulse response sequence. The components of the AR model are already known, as well as the system order N; thus, if an estimate of the first required

Markoff parameters is available, then the calculation of the MA structure is straightforward. For the transducer under impact, we have that even though a considerable proportion of the measured data consists of free-response values, the required first N+1 samples are not available since they are embedded in the forced projectile-transducer interval of contact. In the next section a strategy for dealing with this problem will be discussed.

6.2 Estimation of the required first Markoff parameters

As pointed out before, the problem now consists of estimating the first required Markoff parameters. In essence, a rational structure for the transfer function will be assumed, but its dimension may be larger than the order of the system, in order to counteract the effect of noise and residual crosstalk. It means that p will be larger than N in the following rational structure

$$H(z) = \frac{R(z)}{Q(z)} \qquad (6.5)$$

where

$$Q(z) = 1+q_1 z^{-1}+\ldots+q_p z^{-p}$$

$$R(z) = r_0+r_1 z^{-1}+\ldots+r_p z^{-p}$$

The idea of this procedure is quite simple: an ARMA model of a dimension larger than necessary will be fitted to the Discrete Fourier Transform (DFT) of the system's free response. The over specification, as we have just said, is intended to compensate for residual crosstalk and other perturbations. We are really taking advantage of the

availability of techniques such as the fast Fourier transform algorithm and low pass filtering to obtain the system's free response DFT. Then, for each value of z , we will assume that the complex gain H(z) is available. Later we shall discuss this assumption. Consider the following alternative expression of equation (6.6)

$$\left[1+q_1 z^{-1}+\ldots+q_p z^{-p}\right] H(z) = r_0+r_1 z^{-1}+\ldots+r_p z^{-p} \qquad (6.6)$$

Then, this last equation is valid for each z up to the Nyquist frequency

$$z_k = e^{\frac{2*\pi*j}{N_{data}}}, \quad k = 0\ldots N_{data}-1 \qquad (6.7)$$

For each z_k , $H(z_k)$ is a complex gain available from the DFT. At this point it is important to make an observation. If we take the DFT of our measurement, it is possible to have some intervals in the z domain representing information about the system impulse response, whereas some others represent crosstalk or the impact force itself. It is possible to apply equation (6.6) to relevant frequencies by means of an appropriate windowing process. If so, then we can stack up the equations, which happen to be linear, complex-valued in terms of the values of $\{r_i\}$ and $\{q_i\}$. We have for the most general case

$$F\xi = G \qquad (6.8)$$

where we have implicitly made use of the following matrices

$$G \triangleq \left[H(z_i) \;\; H(z_{i+1}) \;\; H(z_{i+2}) \;\; \ldots \;\; H(z_{i+j})\right]^T$$

$$\xi \triangleq \left[-q_1 \;\; -q_2 \;\; \ldots \;\; -q_p \;\; r_0 \;\; \ldots \;\; r_p\right]^T$$

$$F \triangleq \begin{bmatrix} z_i^{-1}H(z_i) & z_i^{-2}H(z) & \dots & z_i^{-p}H(z_i) & 1, & z_i^{-1} & \dots & z_i^{-p} \\ z_{i+1}^{-1}H(z_{i+1}) & z_{i+1}^{-2}H(z_{i+1}) & \dots & z_{i+1}^{-p}H(z_{i+1}) & 1 & z_{i+1}^{-1} & \dots & z_{i+1}^{-p} \\ z_{i+2}^{-1}H(z_{i+2}) & z_{i+2}^{-2}H(z_{i+2}) & \dots & z_{i+2}^{-p}H(z_{i+2}) & 1 & z_{i+2}^{-1} & \dots & z_{i+2}^{-p} \\ \vdots & \vdots & \vdots & \vdots & \vdots & \vdots & \vdots & \vdots \\ z_{i+j}^{-1}H(z_{i+j}) & z_{i+j}^{-2}H(z_{i+j}) & \dots & z_{i+j}^{-p}H(z_{i+j}) & 1 & z_{i+j}^{-1} & \dots & z_{i+j}^{-p} \end{bmatrix}$$

The matrix F is of size (j)*(2p+1). A least-squares solution for the parameter vector can be obtained if the pseudoinverse for matrix F is found. But under such a calculation it is likely to obtain a complex solution. In order to avoid this difficulty, we take real and imaginary portions of equation (6.8) and construct an auxiliary linear system with real coefficients, so that our solution will certainly be real. Specifically

$$\xi = \left(\begin{bmatrix} re(F) \\ im(F) \end{bmatrix}^T \begin{bmatrix} re(F) \\ im(F) \end{bmatrix} \right)^{-1} \begin{bmatrix} re(F) \\ im(F) \end{bmatrix}^T \begin{bmatrix} re(G) \\ im(G) \end{bmatrix} \qquad (6.9)$$

By restructuring the solution and equating real and imaginary we force the solution of the least-squares optimization to be real. Again, the best fit for the model is given by a product of matrices involving the pseudoinverse of a nonsquare matrix. It is important to point out that, in some sense, the denominator polynomial Q(z) contains information previously obtained in the ARx identification process. In fact, the roots of the ARx model should be included in the set of roots of the polynomial Q.

Now, the last step is to estimate the first N+1 Markoff parameters from the polynomials just obtained. by making use of the convolutional relationship

$$\left(1 + \sum_{j=1}^{p} q_j z^{-j}\right)\left(\sum_{k=0}^{\infty} \overline{h}(k)\, z^{-k}\right) = \sum_{i=1}^{p} r_i z^{-i} \qquad (6.10)$$

The solution of this expression is recursive. We are interested only in the first N+1 values, and , since p>N, we have

$$\overline{h}(0) = r_0$$
$$\overline{h}(1) = r_1 - \overline{h}(0)\, q_1$$
$$\overline{h}(2) = r_2 - \overline{h}(1)\, q_1 - \overline{h}(0)\, q_2$$

and, in general, for any k<p

$$\overline{h}(k) = r_k - \sum_{i=1}^{k} q_i \overline{h}(k-i) \qquad (6.11)$$

The Markoff parameters obtained from equation (6.11) can be inserted into equation (6.4) in order to estimate the components of the MA polynomial. We have assumed that the DFT of the impulse response sequence is available from the fast Fourier transform of the measured signal. It may be that the desired DFT of the system free response is not available due to overlapping effects with other signals. In this case, we can proceed in this way: we can define a fictitious impulse response by shifting the origin to an arbitrary position, neglecting all the information in the past. We calculate the DFT of this fictitious impulse response sequence and proceed estimating a complete ARMA model for it. Then, using this model and the initial conditions in the fictitious impulse response signal, we propagate it backwards in time, so that in some sense we are extrapolating the values of the "true" first Markoff parameters, located at the "true" origin, from a remote

arbitrary position in the future.

6.3 Overall model gain adjustment and deconvolution

The last step in the model identification is the adjustment of the overall gain, in order for the model to yield a force calculation in terms of appropriate units, like Newtons or pounds. There are two gains to be calculated. The first one, called K_u, is intended to make our ARMA model have a low frequency gain of 1. The reason for this is simple. Suppose that we want to measure a "quasi static" force with the transducer. In this case, assuming that the force was applied gradually, the transducer is expected to perform as a dynamometer; that is to say, no vibrations should appear. Therefore, since we don't want distortion in the magnitude of the measurement, the ARMA model should have a unit gain in the low-frequency range. Specifically:

$$|K_u H(z_0)| = 1, \quad for \quad z_0=1 \ (s_0=0).$$

then, we have

$$K_u = \frac{1}{|H(z_0)|}, \quad for \quad z_0=1 \ (s_0=0).$$

The second gain, which we will label K_f, serves the purpose of dimensionalizing the model. It means that this constant will take care of the fact that the force calculation should yield a value in appropriate units such as Newtons or pounds. The manufacturer provides a table of constants that includes the effects of diverse amplifiers and filters as well as other devices, so that the calculations can be carried out in force units.

Now that the transducer model is finally complete, the problem of estimating the impact force becomes a standard filtering process. The vibration measurements will be processed by the algebraic inversion of the ARMA model. Specifically:

$$\sum_{k=0}^{N_c} \bar{u}(k)\, z^{-k} = \frac{\left(1 + \sum_{j=1}^{N} b_j z^{-j}\right)\left(\sum_{k=0}^{N_c} \bar{x}(k)\, z^{-k}\right)}{K_f K_u \left(\sum_{m=0}^{N} a_m z^{-m}\right)} \qquad (6.12)$$

6.4 Synopsis of the identification and deconvolution processes

At this point, it is appropriate to recapitulate the techniques presented and to integrate them in a single body of ordered steps. Figure 6.1 presents a synoptic table of the identification and deconvolution processes, with reference to the relevant texts.

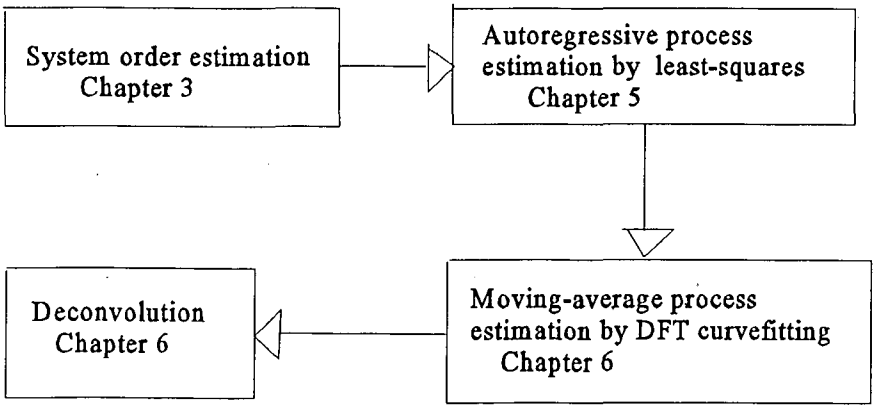

Figure 6.1 Synopsis of the identification and deconvolution methodology

Chapter 7

Numerical Results and Discussion

This chapter presents numerical results for the model identification processes and the calculation of impact forces. A discussion of these results is included. The results will give some insights concerning the events that happen in the impact process.

7.1 Model identification for normal and transverse phenomena

Several experiments were conducted for different impact conditions. The projectile nominal incoming velocities were of 42.67, 36.57, and 30.48 m/s. The angles of incidence with respect to the normal axis were of 15, 25 35 and 45 degrees. The data sampling period is T_s = 3 microseconds.

Figures 7.1 and 7.2 present plots of typical normal and transverse transducer transient measurements respectively. They correspond to an impact process with an incoming projectile velocity of 30.48 m/sec, at an angle of 15 degrees, relative to the normal axis. This set of measurements will be processed in order to identify the models for the transducer. It should be noticed that these measurements are not expressed in any particular units.

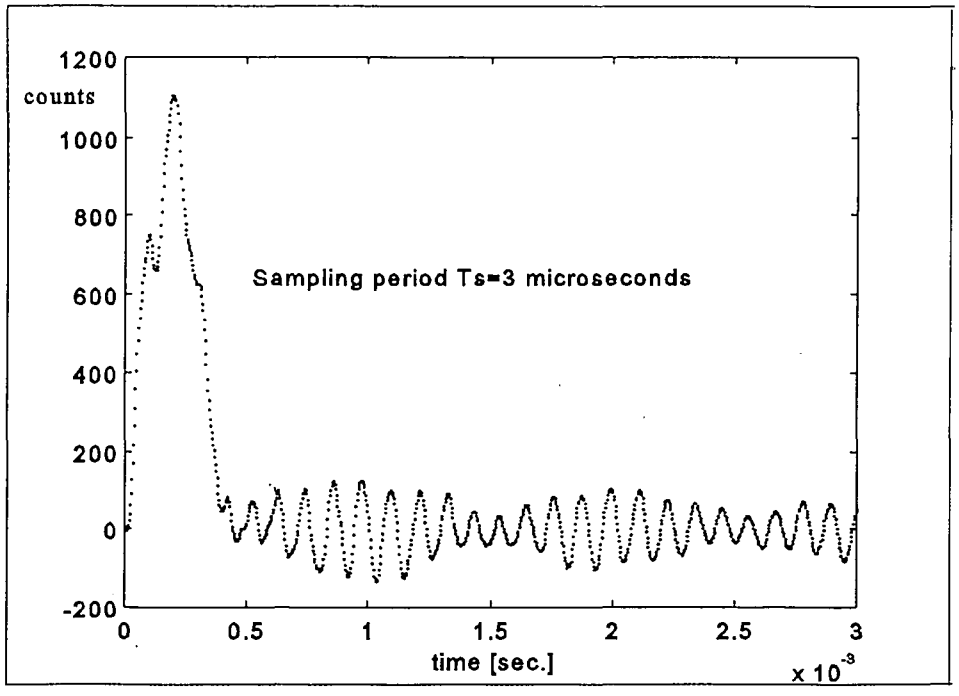

Figure 7.1 Typical normal impact vibration measurements

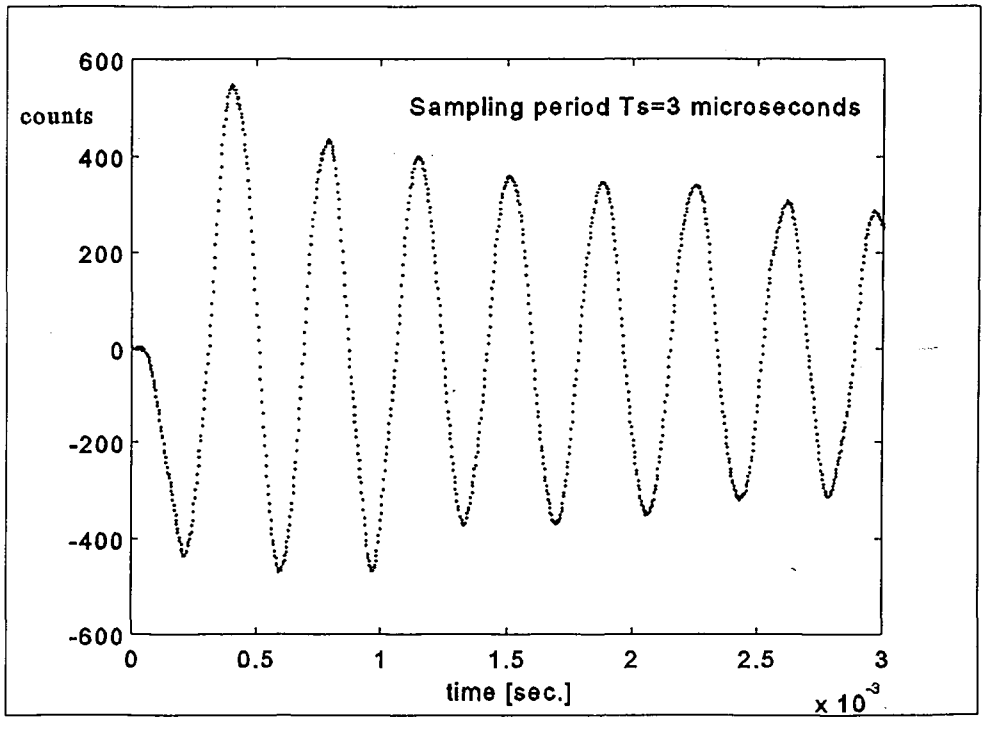

Figure 7.2 Typical transverse impact vibration measurements

A System order estimation for normal and transverse phenomena

The results of the order estimation for both normal and transverse models are presented in figure 7.3. Recall that the algorithm described in Chapter 4 requires the calculation of average determinants for generalized Hankel matrices of different sizes. With these averages, the value of J_p is calculated and plotted in figure 7.3. For both normal and transverse vibrations, the maximum value of Jp occurs at p=4, and thus, the estimate for the order of both models is four.

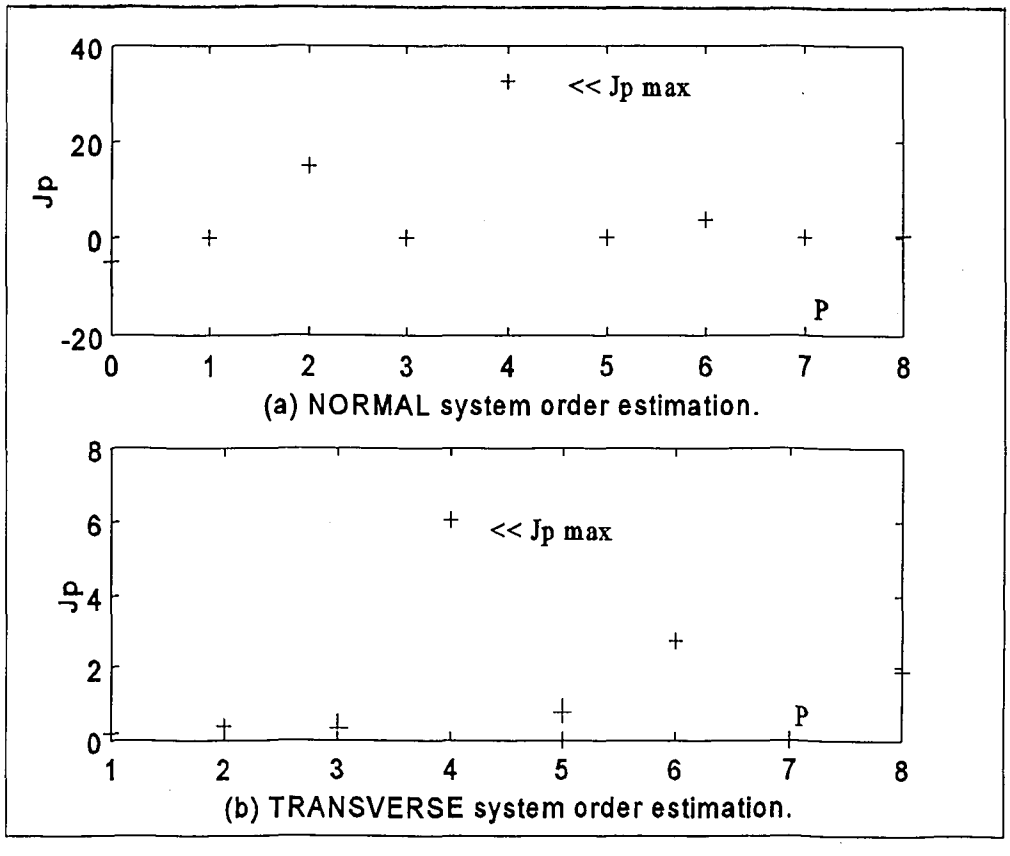

Figure 7.3 System order estimation (normal and transverse)

B System identification for the normal model

The estimation for the normal model order is four, and thus the number of modes that will be modeled is two. These modes correspond to the pair of peaks between the positions 100 and 200 in the signal spectrum of figure 7.4(a). This figure presents the spectra for the signal before and after applying enhancing filters. For the original signal in 7.4(a), we can see that the peak at position 50 corresponds to crosstalk from the transverse channel. Also, there is a high frequency peak at the position 360 that represents an additional low amplitude mode that will not be modeled. In (b) we can see the signal spectrum after isolating the impulse response sequence. This is the information that will be used for ARx identification.

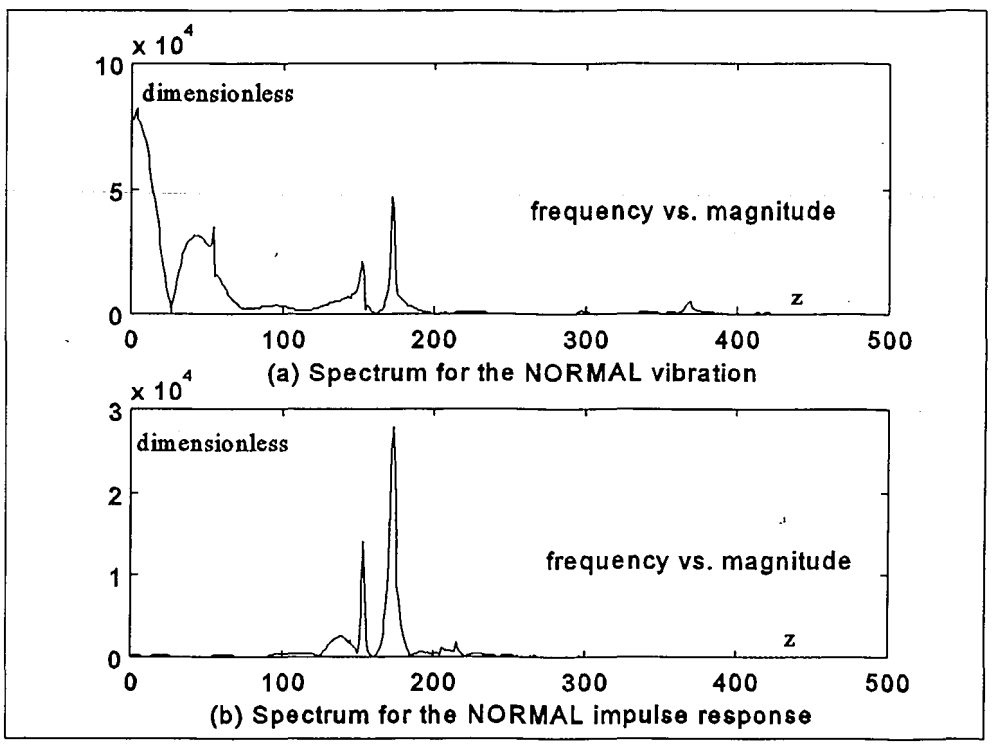

Figure 7.4 Fourier spectra before and after filtering (normal)

Autoregressive process identification

The initial estimation by ordinary least squares, and the subsequent improvements in the estimation are plotted in figure 7.5. The values of each coefficient {b1,b2,b3,b4} converge from the initial ordinary least squares estimate (zeroth iteration) in five iterations.

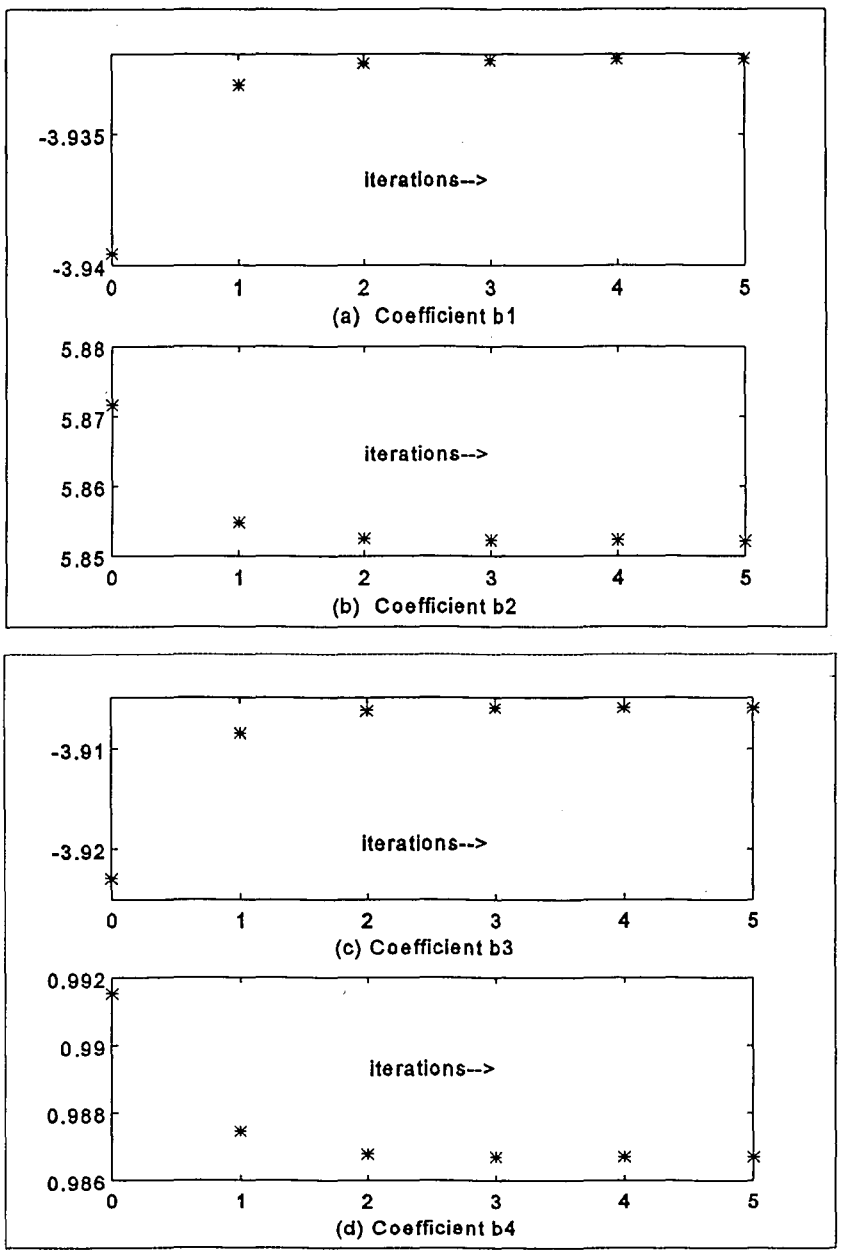

Figure 7.5 Evolution of AR coefficients (normal)

The criterion for convergence is the difference between the k^{th} coefficient and its previous value. The following table presents these differences

	$b_1^k - b_1^{k-1}$	$b_2^k - b_2^{k-1}$	$b_3^k - b_3^{k-1}$	$b_4^k - b_4^{k-1}$
k=1	6.3820000e-03	-1.6678700e-02	1.4443200e-02	-4.0858200e-03
k=2	8.4560000e-04	-2.3345000e-03	2.1612000e-03	-6.6724000e-04
k=3	1.1630000e-04	-3.2290000e-04	3.0070000e-04	-9.3510000e-05
k=4	1.5700000e-05	-4.3700000e-05	4.0600000e-05	-1.2660000e-05
k=5	2.3000000e-06	-6.5000000e-06	6.2000000e-06	-1.9500000e-06

The algorithm was stopped at the fifth iteration, for which the level of error was less than 1.00e-05 . The final AR normal model is

$$1+\sum_{i=1}^{4} b_i z^{-i}=1 - 3.9322z^{-1} +5.8522z^{-2} -3.9060z^{-3} +0.9867z^{-4}$$

with roots inside the unit circle that ensure system stability.

Moving average process identification

The next step is to fit polynomials R(z) and Q(z) to the discrete Fourier transform of the impulse response sequence. Notice that the spectrum for it was isolated successfully by means of conventional digital filters (see figure 7.4 (a) and (b)).

The matrix F and vector G in equation (6.8) were built with information from the FFT presented in figure 7.4(b), and the resulting polynomials R(z) and Q(z) are

$$\frac{R}{Q}=\frac{-83.3475+234.9082z^{-1}-222.6486z^{-2}+70.8864z^{-3}-0.0045z^{-4}}{1 - 3.9265z^{-1} + 5.8309z^{-2} - 3.8806z^{-3} + 0.9768z^{-4}}$$

As we know, this last expression is intended to approximate the impulse response function DFT.

Now, the coefficients of R and Q are used to generate the first five Markoff parameters, by applying formula (6.11). The resulting values are thus inserted in equation (6.4), so that the desired MA parameters are now readily available

$$\begin{bmatrix} a_0 \\ a_1 \\ a_2 \\ a_3 \\ a_4 \end{bmatrix} = \begin{bmatrix} 1 & 0 & 0 & 0 & 0 \\ -3.9322 & 1 & 0 & 0 & 0 \\ 5.8522 & -3.9322 & 1 & 0 & 0 \\ -3.9060 & 5.8522 & -3.9322 & 1 & 0 \\ 0.9867 & -3.9060 & 5.8522 & -3.9322 & 1 \end{bmatrix} \begin{bmatrix} -83.3475 \\ -92.3523 \\ -99.2733 \\ -103.8464 \\ -105.8699 \end{bmatrix}$$

The calculation of parameters a_i is straightforward and leads to the polynomial:

$$\sum_{i=0}^{4} a_i z^{-i} = -83.3475z^{-1} - 223.8926z^{-2} + 71.6046z^{-3} - 0.0072z^{-4}$$

This polynomial has roots inside the unit circle, and thus we know that the system is minimum-phase, so that its algebraic inversion will present no problem.

Normal model gain adjustment

Now, the ARMA model is adjusted so that our calculations are in useful units. First we calculate the low-frequency gain for our ARMA model: it is 348.71 at z=1 (s=0) . Then we divide the MA polynomial by this constant, and our ARMA model will produce net results, in the sense that there will be no amplification. Our final normal ARMA model becomes:

$$\frac{\sum_{i=0}^{4} a_i z^{-i}}{1 + \sum_{i=1}^{4} b_i z^{-i}} = \frac{-0.239 + 0.675z^{-1} - 0.642z^{-2} + 0.2053z^{-3}}{1 - 3.9322z^{-1} + 5.8522z^{-2} - 3.9060z^{-3} + 0.9867z^{-4}}$$

C System identification for the transverse model

The estimation for the transverse model order is four, but it is inconsistent with the number of peaks that we actually find in a signal spectrum (see figure 7.6), The decision was made to assign a model order of two, in order to account for the only peak in the discrete Fourier transform.

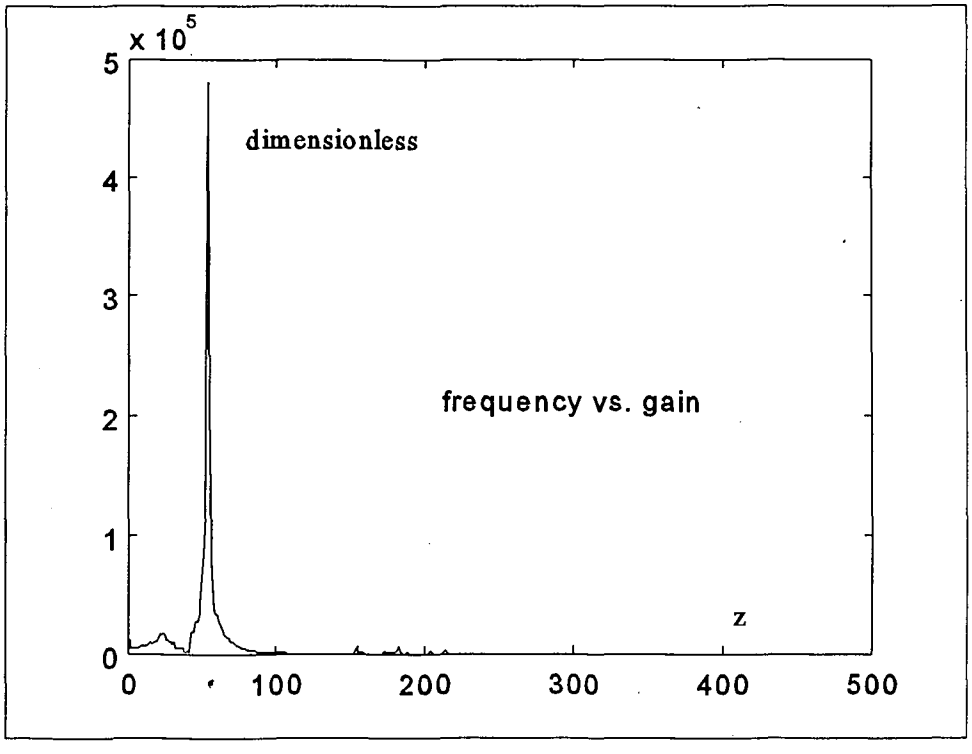

Figure 7.6 Fourier spectrum for the transverse vibration measurements

Autorregressive process identification

The corresponding initial estimation and subsequent improvements are plotted in figure 7.7.The values of each coefficient converge in three iterations. The criterion for convergence is the difference between the i^{th} coefficient and the previous one ,as it was in the

normal ARx identification. These differences are presented in the following table:

	$b_1^k - b_1^{k-1}$	$b_2^k - b_2^{k-1}$
k=1	-9.0200000e-05	1.1177000e-04
k=2	-1.5000000e-06	1.5100000e-06
k=3	-0.2762000e-08	0.3276000e-08

Here, the algorithm was stopped at the third iteration. The level of error is on the order of 1e-08. The final AR transverse model is

$$1 + \sum_{i=1}^{2} b_i * z^{-i} = 1 - 1.9961z^{-1} + 0.9987z^{-2}$$

This polynomial has its roots inside the unit circle, which indicates stability, a condition for the system to have a bounded impulse response sequence.

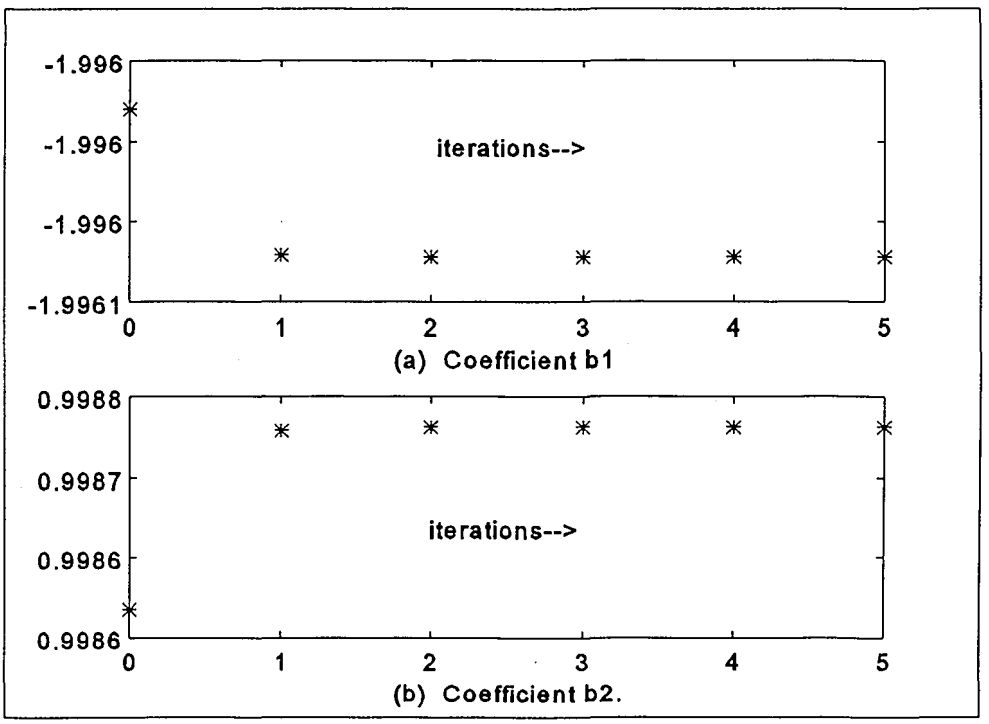

Figure 7.7 Evolution of AR coefficients (transverse)

Moving average process identification

In order to estimate the parameters in the MA model for transverse vibrations, we have to define a fictitious impulse response. This is so because in the spectrum for the original signal it was not possible to isolate the information corresponding to the impulse-response sequence, since it is overlapped with other information. The approach now is to define a fictitious impulse-response sequence, by shifting the origin to an arbitrary location, and to use its DFT to find a complete ARMA model. Then, we can propagate the impulse response backwards in time and thus obtain estimates for the "true" first impulse response parameters, so that we can then obtain the "true" MA polynomial. Figure 7.8 represents the definition of this fictitious impulse response sequence at a maximum of our original signal, so that the origin is shifted by 256 sampling periods. The vertical axis represents dimensionless samples.

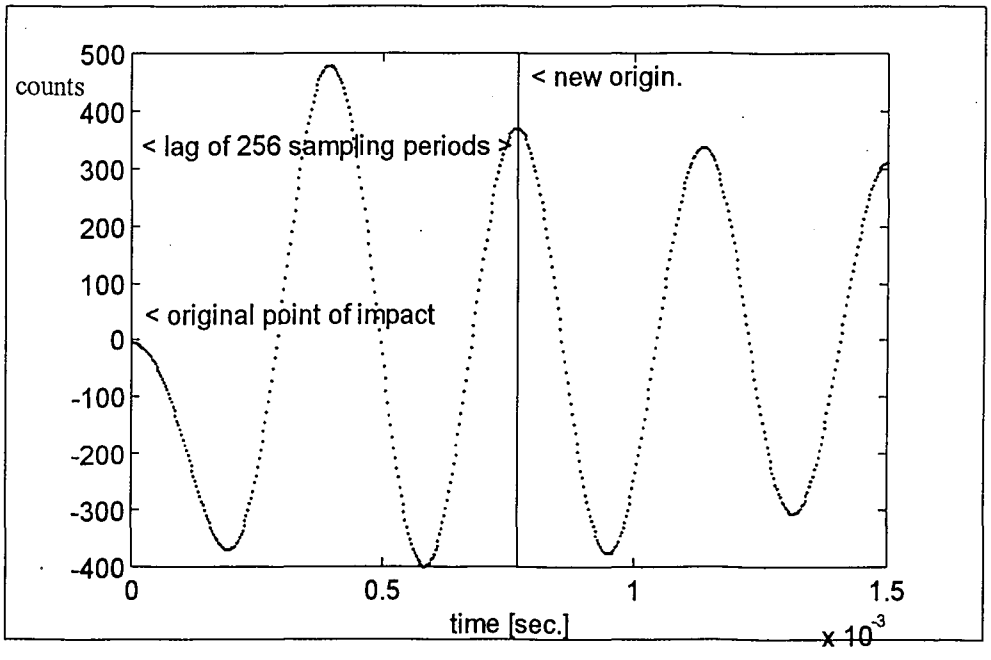

Figure 7.8 Definition of an auxiliary fictitious-impulse response sequence

After curve fitting the DFT of this fictitious sequence, we obtain the following polynomials R(z) and Q(z)

$$\frac{R(z)}{Q(z)} = \frac{-83.3475+234.9082z^{-1}-222.6486z^{-2}+70.8864z^{-3}}{1-3.9265+5.8309z^{-1}-3.8806z^{-2}+0.9768z^{-3}}$$

With these polynomials we estimate the first required Markoff parameters of the fictitious system, and then calculate the corresponding MA polynomial

$$\begin{bmatrix} a_0 \\ a_1 \\ a_2 \end{bmatrix} = \begin{bmatrix} 1 & 0 & 0 \\ -1.9961 & 1 & 0 \\ 0.9987 & -1.9961 & 1 \end{bmatrix} \begin{bmatrix} 341.6761 \\ -329.1879 \\ -0.0074 \end{bmatrix}$$

From this last formula the fictitious MA polynomial is

$$\sum_{i=0}^{2} a_i z^{-i} = 341.6761 - 329.1879z^{-1} - 0.0074z^{-2}$$

Then, we propagate this signal backwards in time, so that an extrapolation of the real first Markoff parameters is obtained. With the required "true" Markoff parameters available, we can estimate the MA polynomial for the real model

$$\sum_{i=0}^{2} a_i z^{-i} = 272.2652 - 251.2036z^{-1} + 0.0000z^{-2}$$

Again, since this polynomial has roots inside the unit circle, we thus know that the transverse model system is minimum-phase, and that its algebraic inversion is feasible.

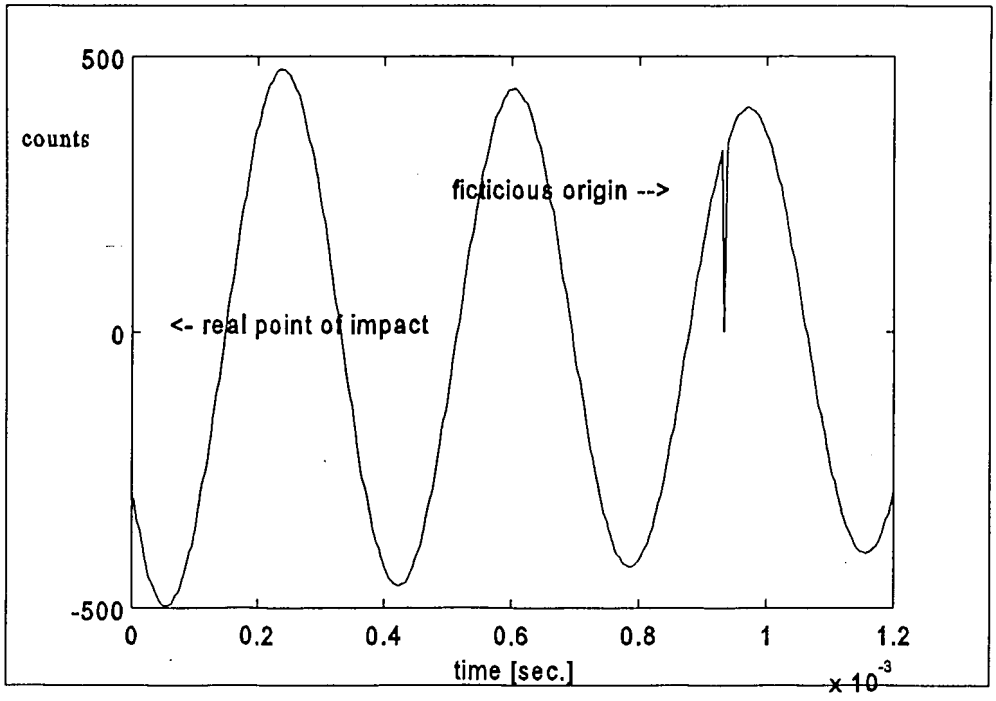

Figure 7.9 Backwards-in-time propagation for the fictitious impulse-response

Model gain adjustment

The transverse ARMA model is also calibrated so that the deconvolution process yields results in useful units. The low-frequency gain of the ARMA transverse model is k=7921.70 at z=1 (s=0). Thus, the final ARMA model that produces no gain distortion in the signal is

$$\frac{\sum_{i=0}^{2} a_i z^{-i}}{1+\sum_{i=0}^{2} b_i z^{-i}} = \frac{0.0344-0.0317z^{-1}}{1-1.9961z^{-1}+0.9987z^{-2}}$$

7.2 Results after filtering the vibrations: impact forces in the transducer

With the complete ARMA models available, the calculation of impact forces becomes an ordinary filtering problem, for which the solution is given by the deconvolutional

relationship given by equation (6.12). The result of such process is presented in what follows.

A Normal impact forces

The experimental data comprised incoming velocities of 42.67m/s, 36.57m/s and 30.48m/s, and incidence angles of 15, 25, 35 and 45 degrees with respect to the normal axis. Figure 7.10 presents three different normal force profiles, for a nominal incoming angle of 15 degrees, for the three different values of initial velocity. Information pertaining to normal impact for a nominal angle of 25 degrees is presented in figure 7.11. In every case, the time of golfball-transducer interaction seems to depend on the incoming velocity. It seems that its value is lower for larger magnitudes of the initial velocity. So, for a more "severe" collision the time of impact is likely to be shorter than for the opposite case.

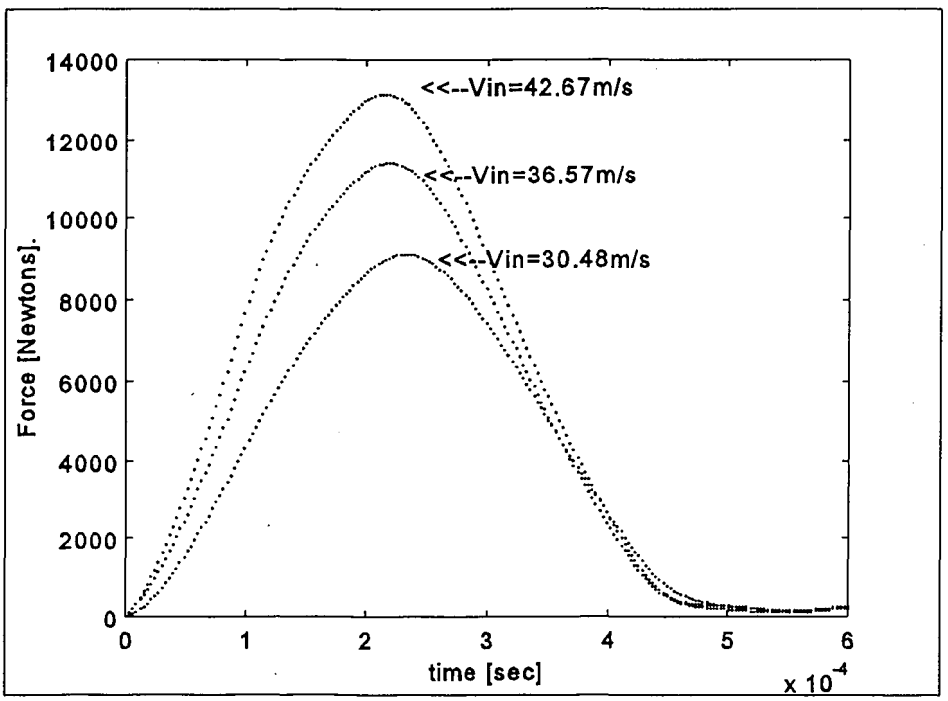

Figure 7.10 Normal impact forces for α=15 degrees

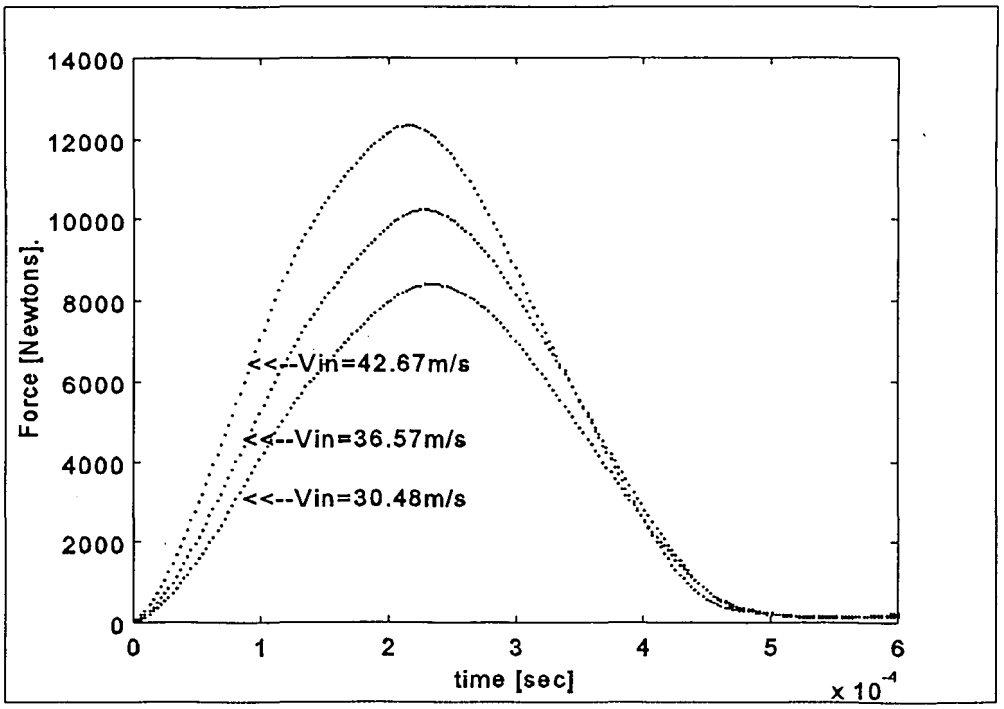

Figure 7.11 Normal impact forces for α=25 degrees

The collision severity depends essentially on the amount of initial ball momentum in the normal direction. Thus, for smaller angles of incidence and larger nominal velocities the normal impact is more intense, and then the impact forces are larger, as can be seen in the plots.

There is more information plotted in figures 7.12 and 7.13, corresponding to angles of 35 and 45 degrees. For any impact experiment, the position of the peak force depends on the collision severity. In general, for a larger amount of initial momentum, the peak force appears slightly to the left, so that the evolution of the phenomenon seems to be faster for a more intense impact. Indeed, larger impact forces imply larger deformation rates in the transducer and in the ball, so that the peak force and the loss of contact will appear to the left for more severe collisions.

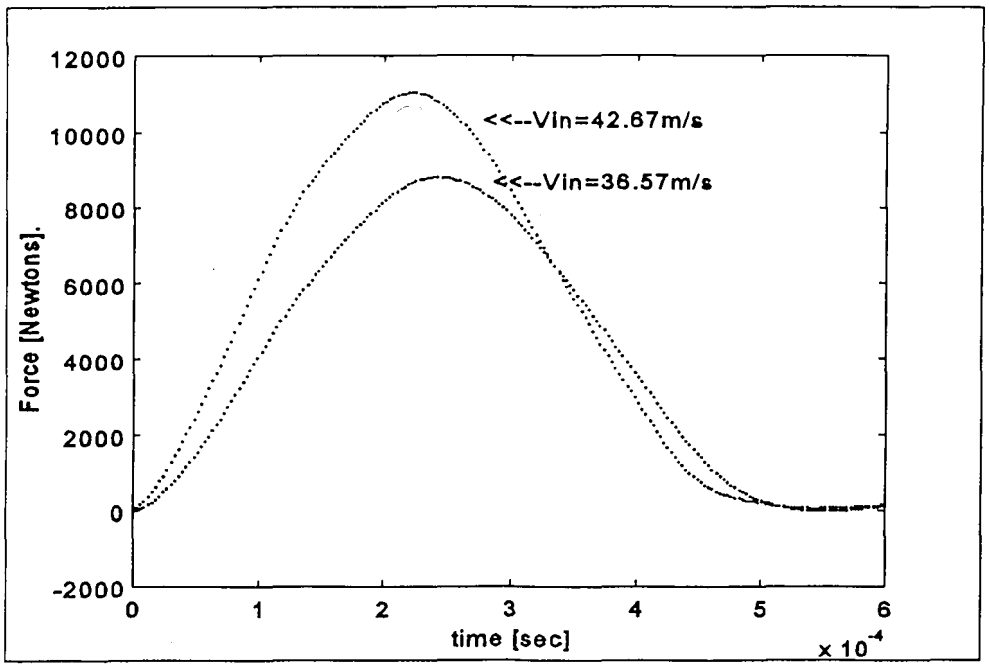

Figure 7.12 Normal impact forces for $\alpha = 35$ degrees

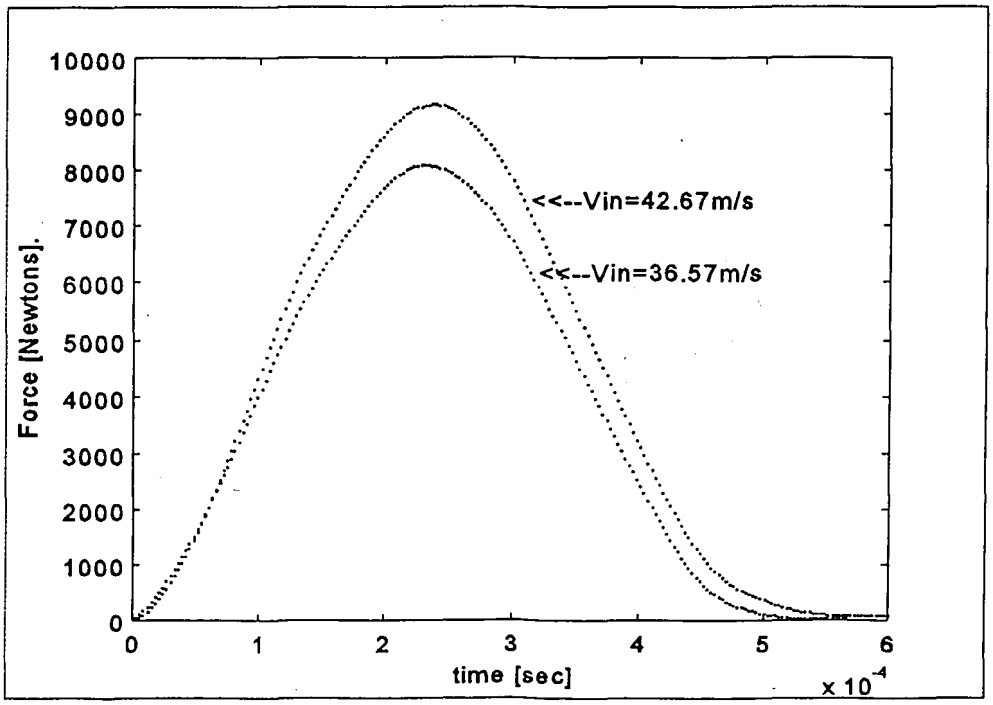

Figure 7.13 Normal impact forces for $\alpha = 45$ degrees

An important observation regarding the characteristic profiles of the normal forces obtained is that there is no change of sign in their interval of validity, as one would intuitively expect. It means that the ball-transducer interaction is only of compressive nature, and this observation gives place to some insights concerning the sequence of events that must take place in the ball. During the interval of time prior to the force peak, the ball experiments increasing deformation, and thus a certain amount of energy is stored in the form of elastic strain. The point of maximum deformation must coincide with the force peak, and during the interval following the maximum, all the energy stored in the form of strain is released again, some to be transferred to the transducer, some to be restored to the kinetic energy of the ball,or converted into heat. These last observations are consistent with the classical conjectures on impact stated by Isaac Newton, in the sense that our measured normal forces indeed present two well-defined intervals of behavior during impact, namely, elastic deformation and restitution, separated by a maximum value in the force profile. In order to test the validity and consistency of the normal impact forces we have just calculated, an index of accuracy must be used.

This index consists of the correlation between the calculated change in momentum and the measured change in momentum. The calculated change in momentum is the integral of the normal impact force with respect to time:

$$\Delta H_{calculated} = \int_{t=o}^{t=t_{LC}} F_N dt$$

The measured change in momentum is obtained from measurements of the actual incoming

and outgoing velocities, and the actual angles of incidence and rebound

$$\Delta H_{measured} = m[\ V_0 \cos(\alpha_0) + V_1 \cos(\alpha_1)\ ]$$

Figure 4.14 presents these results for 27 different experiments. The error never exceeded 4.5%, which says that our calculations are reasonably accurate.

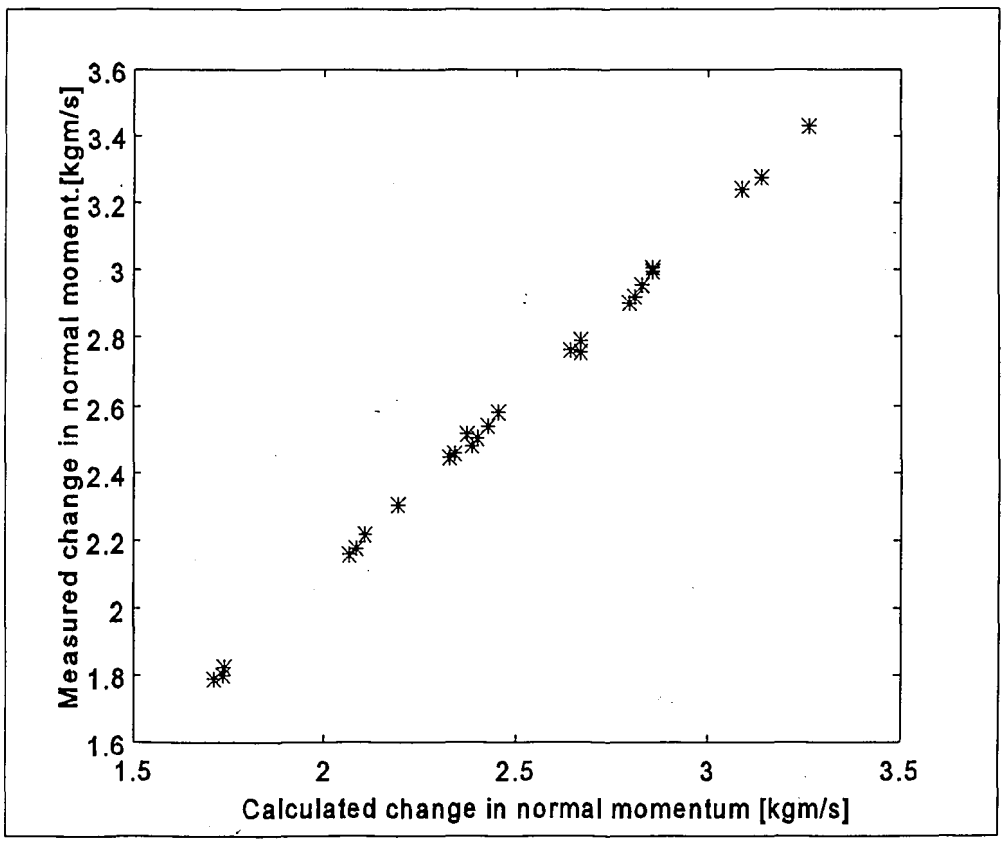

Figure 7.14 Calculated vs. measured change in normal momentum [kg*m/s]

B Transverse impact forces

Figure 7.15 contains typical results for low intensity transverse impact. We can observe in this plot that there is a sign reversal in the force profile, in opposition to the normal case where the force does not cross the horizontal axis during the impact process. Another important observation is that the peak force appears sooner for a smaller amount of initial transverse momentum, so that the force maximum for an angle of 15 degrees appears to the left with respect to the case of 25 degrees. Similar profiles appear in figure 7.16, where the incoming velocity is of 36.57 m/s. Notice that, as the intensity of the impact increases, the negative portion of the force profile becomes smaller.

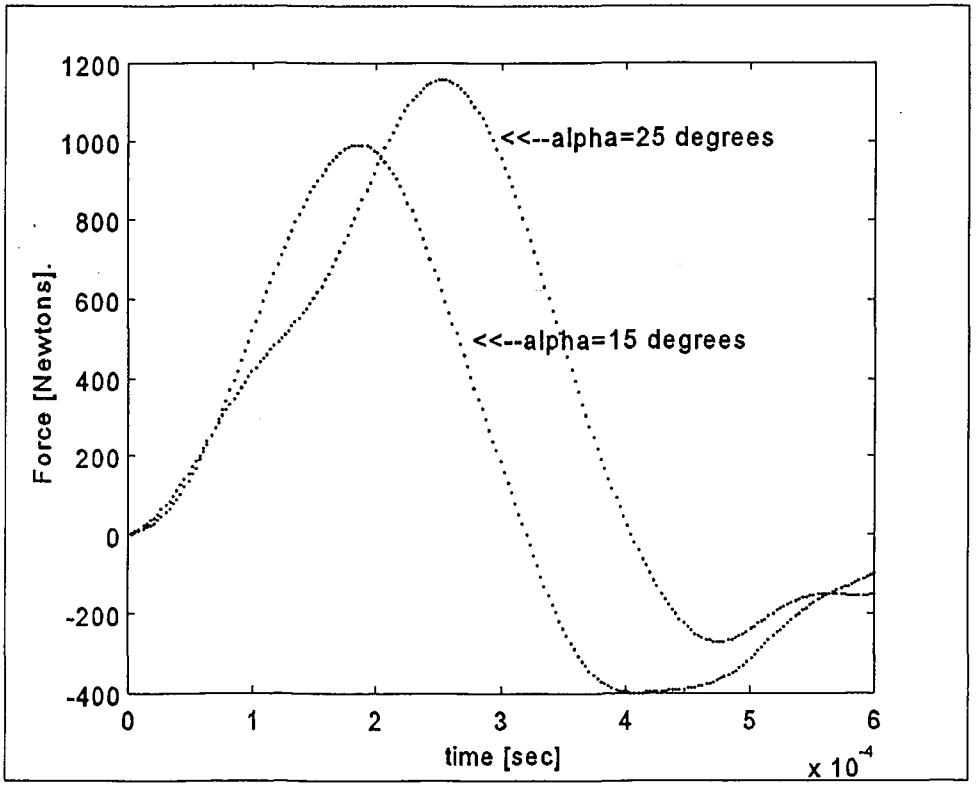

Figure 7.15 Transverse impact forces for Vin=30.48 m/s

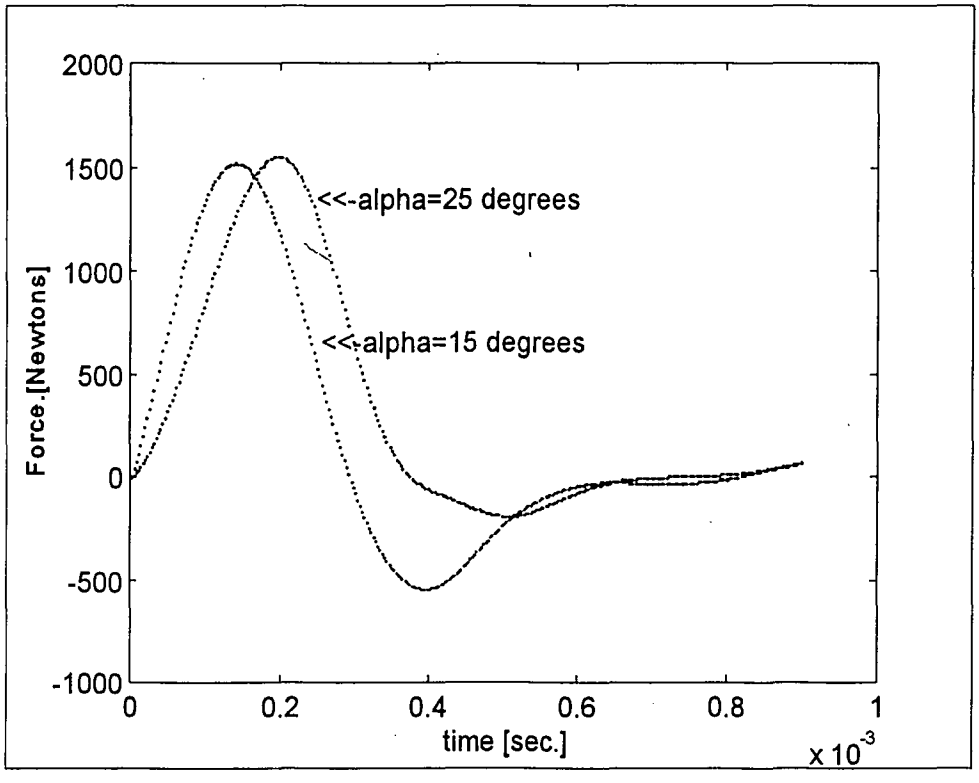

Figure 7.16 Transverse impact forces for Vin=36.57 m/s

More experimental information is depicted in figure 7.17, now for an incoming velocity of 36.57m/s, and larger angles of incidence. The initial transverse momentum is larger than those of figures 7.15 and 7.16. We notice that the negative portion of the curves has decreased significantly, so that most of the transverse force is positive. In fact, as the transverse impact becomes more and more intense, the negative portion of the force

profiles tends to disappear. Incidentally, for the cases plotted in figure 7.18, the impact forces are essentially positive.

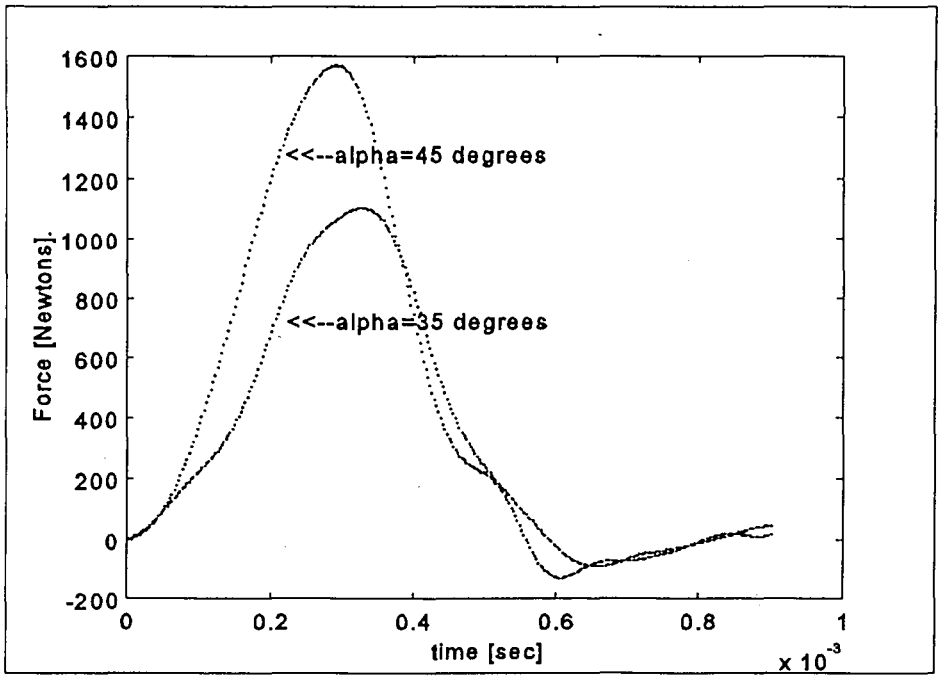

Figure 7.17 Transverse impact forces for Vin=36.57m/s

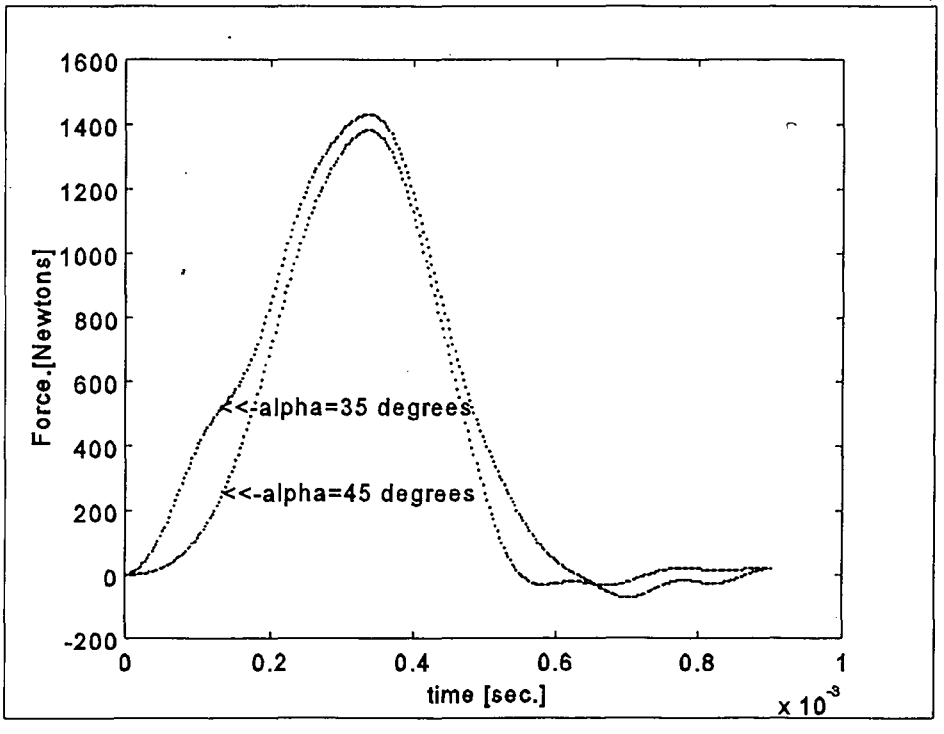

Figure 7.18 Transverse impact forces for Vin=42.67m/s

A test of validity analogous to that of normal impact forces was applied to the transverse impact data. The calculation of change in transverse momentum is nothing but the time integral of the corresponding impact force, whereas the measured change in momentum is estimated from measurements of incoming and outgoing velocities, angles, and final spin rate. Figure 7.19 contains such comparison for the eight experiments that have been previously presented. The error never exceeded 6%.

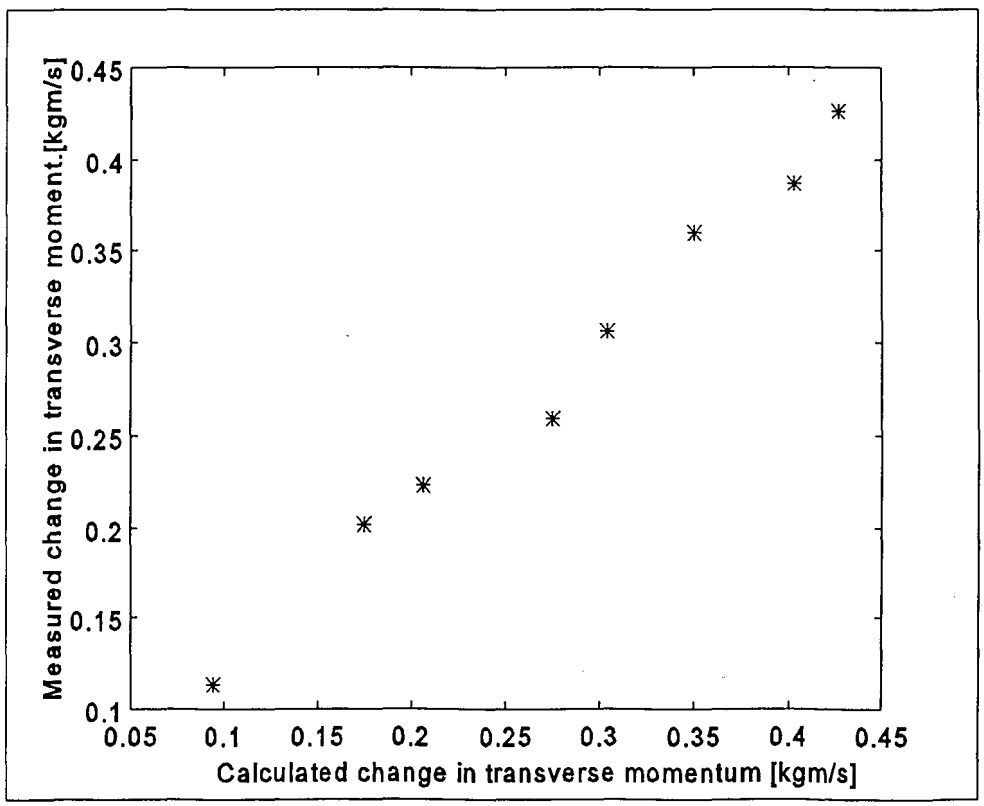

Figure 7.19 Calculated vs. measured change in transverse momentum [kg*m/s]

Some remarks are relevant at this point concerning the consistency and validity of the transducer models. It is evident that there is no consistency between the normal and transverse forces, since the former last for periods of about 460 microseconds, whereas

the latter seem to last for about 600 or 700 microseconds. This happens because the transverse model does not represent the transducer behavior appropriately. Essentially, an ARMA model proved to be inadequate modeling transverse impact vibrations. A nonlinear model should be used in order to account for the sluggish behavior in the transverse channel, including the potential effect that Coulomb friction may have on it, as a result of relative displacement between quartz discs and the steel plate surface. This sluggish behavior of the transducer and the consequent delay in the transverse force profile have been reported by several researchers (e.g., Gobush [22]). A possible solution to this problem may be a redesign of the transducer structure intended to increase its natural frequency by subtracting mass from the upper steel plate, so that its responsiveness to the high-rate evolution of transverse impact forces is adequate. Another solution consists of modeling the transverse vibrations with a nonlinear model, including the effects of hysteresis and lag resulting from the relative displacements that have been mentioned before. The redesign of the transducer structure would be preferred to the analytical approach, since the selection of a nonlinear model and its identification are not easy tasks. It is important to notice that, despite the apparent lag in the transverse forces, the change in momentum calculated on the basis of those profiles is consistent with the measured change in momentum, as shown in figure 7.19. It means that, even though the transverse profiles are not valid, we can still evaluate the change in momentum by integrating them with respect to time.

The ARMA model for normal impact, on the other hand, performed the deconvolution appropriately and resulted in normal force profiles that make physical sense: they are

strictly positive, implying the compressive nature of the normal impact process, and they present two well-defined stages in the impact process, namely, initial compression and restitution.

Chapter 8

Conclusions and future research

8.1 Summary of conclusions

This chapter presents some guidelines intended to improve the numerical results and enhance the data processing. It is relevant to summarize the results and conclusions presented in Chapter 7. Two independent ARMA models were constructed for normal and transverse phenomena in the transducer. Then, these models were used for estimating the true impact force profiles by means of a deconvolutional process. The identification of the models involved parameter estimation by means of least-squares schemes in time and in the frequency domain.

The resulting normal impact force profiles were reasonably good. It was found that the time of interaction between the projectile and the transducer decreases as the impact intensity increases. Also, the maximum value in the normal force profile seems to appear earlier for larger impact intensities. So, in general it can be stated that the sequence of events becomes faster for larger values of momentum involved in the process. The correlation between the calculated and the measured change in normal momentum was very high, indicating that the normal impact forces are valid. The normal model represented the transducer dynamics reasonably well.

On the other hand, the transverse model did not represent the transducer dynamics

appropriately. A common feature of the transverse impact forces calculated with the ARMA model is lag or delay in its evolution, since the time of loss of contact for transverse forces is larger than for normal forces. The reason for this apparent sluggish behavior in the transverse channel seems to be related with the transducer configuration. The transducer's original design was altered, incorporating an additional steel plate attached to the upper surface intended to protect it from the intense impact forces. This plate is essentially an additional mass that makes the natural frequencies of the apparatus decrease significantly, and as a consequence, its responsiveness to high-velocity phenomena is compromised.

The transducer behavior in normal impact was not significantly affected, probably due to the compressive nature of the normal force, which is entirely transmitted to the corresponding quartz disc, leaving no delay or lag of any kind. On the other hand, the transverse behavior may have been drastically changed. Recall that the transverse force is transmitted from the upper steel plate to the corresponding quartz disc by means of shear and friction between surfaces in contact. It is conjectured that under impulsive transverse forces, a relative displacement between the upper steel plate and the upper quartz disc may appear in some intervals of the impact process. It would in turn produce nonlinear behavior that cannot be represented by the proposed model for the transverse channel.

8.2 Future research

It has been pointed out in the summary of conclusions that the transverse model did not represent the dynamical behavior of the transducer appropriately, and that this was due to

nonlinearities arising from the presence of friction and relative displacements between plates when impulsive transverse forces are applied to the structure. The most important nonlinear effect of friction in the transverse model is hysteresis. It is possible to deal with the problem by establishing a nonlinear model for the transverse channel and incorporating hysteresis into it. But even though there are several techniques for nonlinear system identification, a common required condition is that the nonlinearity be differentiable in the interval of validity. The model for hysteresis has a discontinuity at the position x'=0 in the derivative of the relationship F= F(x'), and this is why an analytical approach to the transverse nonlinear modeling problem has a serious drawback.

A pragmatic approach to the problem, proposed by Gobush [22], consists of redesigning the transducer, so that the additional plate intended to protect it has the minimum possible amount of mass, and its addition to the apparatus does not decrease the system natural frequencies significantly. Also, the redesign may consist of a modification in the assembly such that the transmission of the transverse force is not by friction, but by shear only.

If the transducer redesign succeeds in eliminating nonlinear phenomena in the transverse model, then an overall ARMA model can be constructed to represent the transducer with a single, multi variable structure, comprising the coupled effect that each channel has on the other (crosstalk). Recall that in the present work, the crosstalk was eliminated by means of enhancing low-pass filters, and it made possible the construction of independent univariable models for normal and transverse dynamics respectively. The following equation represents this idea

$$\begin{bmatrix} x_N \\ x_T \end{bmatrix} = \begin{bmatrix} H_N & H_{NT} \\ H_{TN} & H_T \end{bmatrix} * \begin{bmatrix} u_N \\ u_T \end{bmatrix} \qquad (8.1)$$

: Here, the ARMA model is multi variable, and the terms off the diagonal in the square matrix represent crosstalk effects between channels. Thus crosstalk becomes part of the model instead of being an internal perturbation in the signals. A practical problem arises in a multi variable , frequency-domain approach, namely, how to calculate the spectra of the cross-transfer functions H_{NT} and H_{TN}, from the information available.

Another improvement in the identification techniques is the following one. Suppose that the AR model has been calculated. Recall equation (6.5)

$$H(z) = \frac{R(z)}{Q(z)} \qquad (6.5)$$

If the order of the polynomials R(z) and Q(z) is set to be equal to the system order, then the polynomial Q(z) can be replaced by the AR polynomial, for which the coefficients are already known. This substitution decreases the number of parameters to be estimated in the discrete Fourier transform curve-fitting. Specifically, only the polynomial R(z) will remain unknown. Moreover, the polynomial R(z) will be an estimation of the MA polynomial. The problem is that, by decreasing the order of R(z) we no longer account for noise or any perturbation, and thus the estimation will be rather poor. An iterative scheme should be investigated to improve the estimation in this case.

References:

[1] Jones, N. (1989). Structural Impact. Cambridge, England. Cambridge University Press.

[2] Juang, J.N. (1974). Applied System Identification. Englewood Cliffs, New Jersey. Prentice Hall.

[3] Hamouda, A.M.S., Hashmi,M.S.J. (1992).Simulation of the impact of a tool steel projectile into copper, mild steel and stainless steel test specimen. Proceedings of the Second International Conference on Structures under Shock and Impact. Portsmouth, U.K.

[4] Kuo, B. (1980). Digital Control Systems. New York, N.Y. Holt, Rinehart and Winston, Inc.

[5] Lee, R.C.K. (1970). Optimal Estimation, Identification and Control. Cambridge, Massachusetts. The MIT Press.

[6] Zhu, Y.Y., Cescotto, S. (1992). A fully coupled elastoplastic damage modeling of contact-impact between two deformable bodies. Proceedings of the 2nd International Conference on Structures under Shock and Impact. Portsmouth, U.K.

[7] Papoulis, A. (1991). Probability, Random Variables and Stochastic Processes. New York, N.Y., McGraw Hill.

[8] Tao, J.R., Krimorat, A., Sun, K. (1992). Modeling of lateral collision between

adjacent structures. Proceedings of the Second International Conference on Structures under Shock and Impact. Portsmouth, U.K.

[9] Ljung, L.(1987). System Identification,: Theory for the User. Englewood Cliffs, New Jersey. Prentice Hall.

[10] Zukas, J.A., Nicholas,T., Swift,H.,Greszczuk, L., Curran,D. (1981) Impact Dynamics. New York,N.Y., John Wiley and Sons.

[11] Arnaudeau, F., Dubois, J. (1984). Numerical techniques and experimental validations for industrial applications. London, U.K. Proceedings of the International Conference on Structural Impact and Crashworthiness.

[12] Greenwood,D.T. (1988). Principles of Dynamics. Englewood Cliffs, New Jersey. Prentice Hall.

[13] Brach, R.M. (1991). Mechanical Impact Dynamics, Rigid Body Collisions. New York, N.Y. John Wiley and Sons.

[14] Samuelides, E., Frieze, P.A. (1984). Analytical and numerical simulation of beams subjected to impact. London, U.K. Proceedings of the International Conference on Structural Impact and Crashworthiness.

[15] Beer,F.P., Johnston, E.R. (1984). Vector Mechanics for Engineers, Dynamics. New York, N.Y. McGraw Hill.

[16] Kinslow, R. (ed.) (1970). High Velocity Impact Phenomena. New York, N.Y. Academic Press.

[17] Zukas, J.A. (ed.) (1990) High Velocity Impact Dynamics. New York, N.Y. John Wiley and Sons

[18] Chow, P.C., Yang, L.J., Gobush, W. (1994). Contact forces, coefficient of restitution, and spin rate of golf ball impact. London, England. Proceedings of the World Scientific Congress of Golf.

[19] Ujihashi, S. (1994). Measurement of dynamic characteristics of golfballs and identification of their mechanical models. London, England. Proceedings of the World Scientific Congress of Golf.

[20] Lieberman, B.B., Johnson, S.H. (1994). An analytical model for ball-barrier impact. Part 1.- Models for normal impact. London, England. Proceedings of the World Scientific Congress of Golf.

[21] Lieberman, B.B., Johnson, S.H. (1994). An analytical model for ball-barrier impact. Part 2.- A model for oblique impact. London, England. Proceedings of the World Scientific Congress of Golf.

[22] Gobush, W. (1990). Impact force measurement on golf balls. St. Andrews, Scotland. Proceedings of the First World Scientific Congress of Golf.

[23] Lieberman, B.B. (1990). The effect of impact conditions on golf balls. St. Andrews, Scotland. Proceedings of the First World Scientific Congress of Golf.

[24] Sinha, N.K., Kuszta, B. (1983). Modeling and Identification of Dynamic Systems. New York, N.Y. Van Nostrand Reinhold Company.

[25] Bayard, D.S., (1994). An algorithm for State Space Frequency domain Identification without windowing distortions. Pasadena, California. IEEE Transactions on Automatic Control.

[26] Hsia, T.C. (1976). On least squares algorithms for system parameter

identification. IEEE Transactions on Automatic Control.

[27] Clarke, D.W. (1967).Generalized least-squares estimation of the parameters of a dynamic model. Proceedings of the IFAC Symposium on Identification in Automatic Control Systems.

[28] Chow, J.C. (1971). On the estimation of the order of a Moving Average process. IEE. Transactions on Automatic Control.

[29] Woodside, C.M. (1971). Estimation of the order of linear systems. Automatica. vol. 7, pp 727-733.

[30] Astrom, K.J., Eykhoff, P. (1971). System Identification-A survey. Automatica. vol. 7, pp 123-162.

Appendix A

Experimental methods

This section is intended to describe the experimental procedures used to take measurements of the impact process variables. Figure A.1 contains all the variables that are used to characterize the golf-ball dynamics before and after the impact.

V_0= golf-ball incoming velocity.

V_1 = golf-ball rebound velocity.

α_0= initial angle of approach.

α_1=final angle .

ω_0=initial spin rate. (In general it is assumed to be zero).

ω_1=final spin rate.

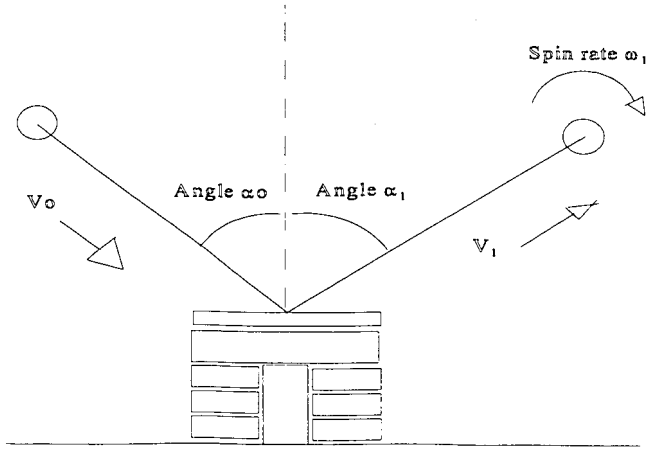

Figure A.1 Definition of variables

Figure A.2 presents the measurement of velocity. Two parallel sheets of light, separated by a distance D, are placed in a region of space containing the golf-ball trajectory. As the ball crosses the first sheet of light, it triggers the measurement of time elapsed to cross the region between the sheets of light, which will be labeled t_o. Since the angle of the velocity vector α and the distance D are known, an estimation of the velocity V is readily obtained from the expression

$$V = \frac{D}{t_c \cos(\alpha)}$$

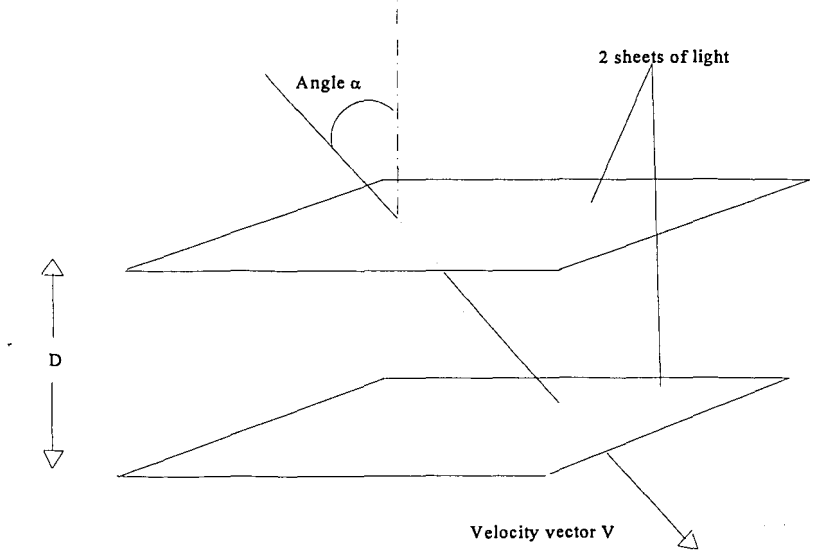

Figure A.2 Measurement of velocity

Figure A.3 describes the measurement of trajectory angles. The initial angle α_0 is known since it corresponds to the orientation of the air cannon. The final angle α_1 is measured in this way: after the ball has collided with the transducer, it in turn hits a sheet of paper, and the point where the hole is located is used to estimate the corresponding angle.

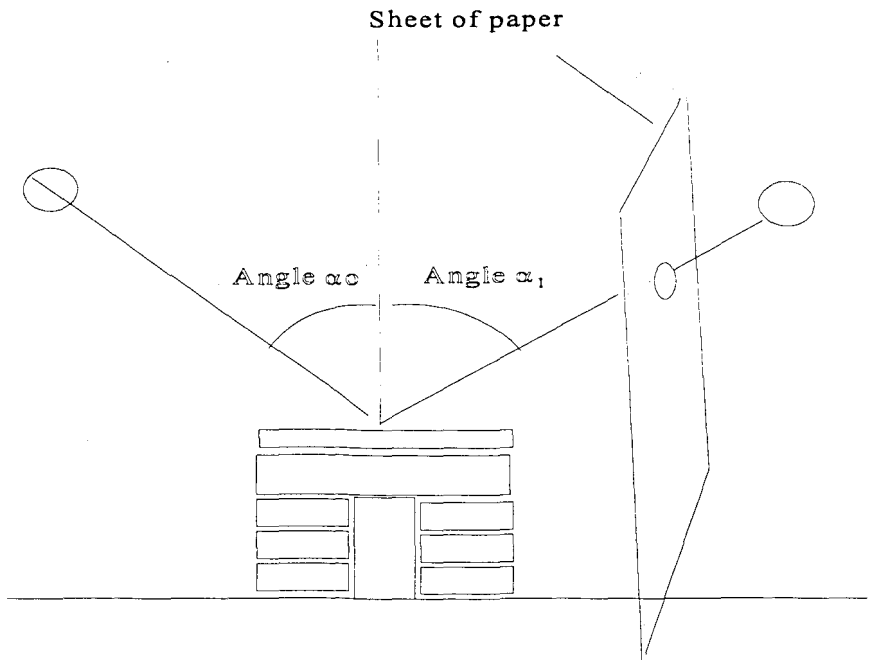

Figure A.3 Measurement of trajectory angles

Figure A.3 illustrates the measurement of spin rate. The initial spin rate ω_0 is supposed to be zero. The final spin rate ω_1 is estimated by means of a stroboscopic process. Essentially, a set of black dots are marked on the ball surface. Once the ball has collided with the transducer, a photographic camera is activated twice, and the time elapsed between the shots is known. When the pictures are processed, careful measurements are taken and fed into a computer program that estimates the spin rate from this information.

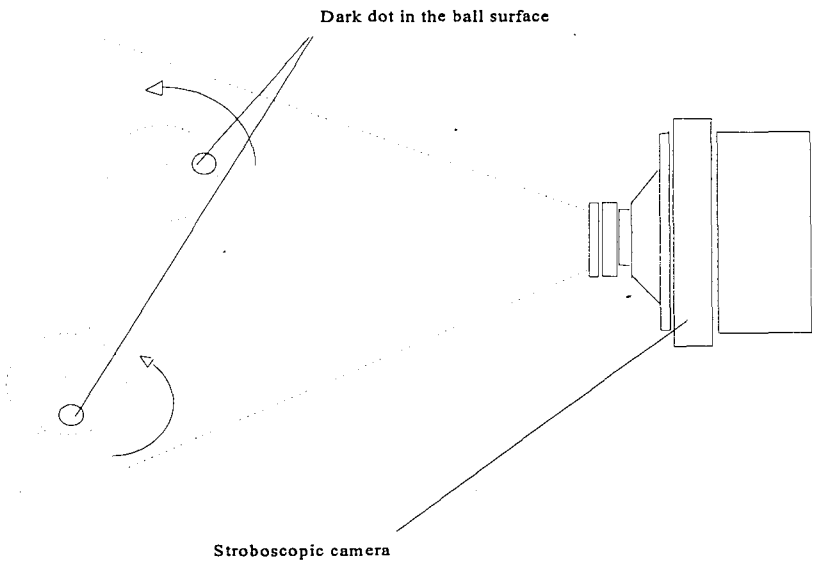

Figure A.4 Measurement of spinrate

Vita

Ruben T. Huerta Ochoa was born in Mexico City on May 25, 1971, he is the third child of Maria del Carmen Ochoa Santoyo and Juan Manuel Huerta Sandoval. He completed his elementary and middle education at the Colegio Mexico and his pre-college studies at the Centro Universitario Mexico, both in Mexico City. He obtained a B.S. in mechanical and electrical engineering in December 1993 from the Instituto Tecnologico de Monterrey, Mexico State Campus. After his graduation he spent one semester as an instructor of mathematics for high school students.

Mr. Huerta Ochoa was awarded a Fulbright-Garcia Robles scholarship by the National Council of Science and Technology (CONACyT, Mexico) and the Institute of International Education (IIE, New York), to pursue graduate studies in mechanical engineering at Lehigh University. He is member of the Phi Beta Delta Honor Society for International Scholars. His long-term career purpose is to devote his efforts to educate new generations of engineers in Mexico and to contribute to the development of his country by applying science and technology to the solution of the severe social and economical problems that affect his fellow Mexicans. By doing so, he hopes to pay back for the many privileges and opportunities he has received throughout his life.

END OF TITLE